# DEVELOPMENT OF A HIGHLY SENSITIVE GOGGLE FOR FLUORESCENCE-BASED DETECTION OF MIDDLE EAST RESPIRATORY SYNDROME CORONAVIRUS (MERS-CoV) AND OTHER PATHOGENS

**YANG LIU, PhD, PI**
**MANUEL Y. CABALLERO, CIV**
**THO HUA, CTR**

**FINAL REPORT**

**AUGUST 2020**

**59th Medical Wing**
**Office of the Chief Scientist**
**1632 Nellis Street, Bldg., 5406**
**JBSA-Lackland, TX 78236**

**DISTRIBUTION A. Approved for public release; distribution is unlimited.**

***DECLARATION OF INTEREST***

*The views expressed in this article are those of the authors and do not necessarily reflect the official policy or position of the Department of the Air Force, Department of Defense, nor the U.S. Government. This work was funded by Project Code Number AC12EM01. Authors are military service members, employees, or contractors of the US Government. This work was prepared as part of their official duties. Title 17 USC §105 provides that 'copyright protection under this title is not available for any work of the US Government.' Title 17 USC §101 defines a US Government work as a work prepared by a military service member, employee, or contractor of the US Government as part of that person's official duties*.

*The views of Thermo Fisher Scientific are not necessarily the official views of, or endorsed by, the U.S. Government, the Department of Defense, or the Department of the Air Force. No Federal endorsement of Thermo Fisher Scientific is intended.*

**NOTICE AND SIGNATURE PAGE**

Using Government drawings, specifications, or other data included in this document for any purpose other than Government procurement does not in any way obligate the U.S. Government. The fact that the Government formulated or supplied the drawings, specifications, or other data does not license the holder or any other person or corporation or convey any rights or permission to manufacture, use, or sell any patented invention that may relate to them.

Qualified requestors may obtain copies of this report from the Defense Technical Information Center (DTIC) (http://www.dtic.mil).

**DEVELOPMENT OF A HIGHLY SENSITIVE GOGGLE FOR FLUORESCENCE-BASED DETECTION OF MIDDLE EAST RESPIRATORY SYNDROME CORONAVIRUS (MERS-CoV) AND OTHER PATHOGENS**

Ruben O'Neal

BRINKLEY.CARLTON.CLARENCE.JR.1048285950
Digitally signed by BRINKLEY.CARLTON.CLARENCE.JR.1048285950
Date: 2020.09.03 14:14:26 -05'00'

RUBEN O'NEAL III, DAF
Medical Modernization Program Analyst
Human Performance & Force Health Protection
59th Medical Wing – Science & Technology

CARLTON C. BRINKLEY, Ph.D., DAF
Dir., Diagnostics & Therapeutics Research
59th Medical Wing – Science & Technology

This report is published in the interest of scientific and technical information exchange, and its publication does not constitute the Government's approval or disapproval of its ideas or findings.

**PAGE LEFT INTENTIONALLY BLANK**

**Development of a Highly Sensitive Goggle for Fluorescence-Based Detection of Middle East Respiratory Syndrome Coronavirus (MERS-CoV) and Other Pathogens**

Manuel Y. Caballero[1], Tho Hua[1]and Yang Liu, PhD[2]

[1]US Air Force, 59th Medical Wing, Science & Technology, JBSA-Lackland, San Antonio, Texas 78236

[2]University of Iowa, Department of Electrical and Computer Engineering, Iowa City, IA 52242

**KEYWORDS**

Multipurpose Imaging Goggle, MERS-CoV, fluorescence, antibody

**"**The views expressed are those of the author's and do not reflect the official views or policy of the Department of Defense or its Components"

**ABSTRACT**

In this project, a fluorescence-sensitive goggle prototype was developed at the University of Akron with potential field applicability in detection and identification of viral and bacterial pathogens. The goggle prototype is a wearable device that has two lenses for capturing 3D stereoscopic images. It also has video-recording capability. Further, an especially important feature of the goggle is that it can transmit the information back to a computer for detailed analysis. At the Center for Molecular Detection (CAMD), our work focused on testing and evaluation of the goggle's fluorescence detection capability. To do that, we devised an *in vitro* fluorescence-linked immunosorbent assay (FLISA). For this assay, we used purified spike protein of Middle East Respiratory Syndrome Coronavirus (MERS-CoV) and several anti-spike protein polyclonal and monoclonal antibodies. The fluorescent dye Alexa Fluor® 647 conjugated to secondary antibodies was used as the fluorophore. For comparison, the fluorescence signals were also read with a BioTek plate reader. The goggle prototype was able to detect fluorescence signals with detection limit of 625 ng/mL of the Alexa Fluor® 647 goat anti-rabbit IgG in a 96-well plate format. For the detection of purified MERS-CoV spike protein, samples with the spike protein can be distinguished from samples without the spike protein. However, the fluorescence detection limit was significantly lower in comparison to the fluorescence detection limit of the BioTek plate reader in 96-well plate format. The software for the goggle prototype was easy to use and offered several options to improve the quality of the capture images and the detection limit of the fluorescence signal.

## INTRODUCTION

With worldwide outbreaks of emerging and reemerging infectious disease agents, such as Ebola virus, Chikungunya virus, Zika virus, and the recent Coronaviruses (MERS-CoV, SARS-CoV, SARS-CoV-2), early detection and identification of these agents is of high priority. Detection and accurate identification of deadly pathogens at the sites or areas where they first emerge is of pivotal importance, as it allows early epidemiologic planning to limit and control the spread of the pathogens. For on-site detection and identification, small, portable, hand-held, real-time devices that have high sensitivity and specificity would be extremely useful. The development of such devices has been a high priority for the Department of Defense (DoD), especially since the anthrax spore attacks via surface mail in 2001 (1). The recent sudden emergence of the SARS-CoV-2 in China and its rapid subsequent spread all over the World further underscores the DoD priority to expeditiously identify such deadly pathogens where they first emerge.

This project aimed to develop a small, hand-held, light, fluorescence-sensitive, portable goggle device that can be carried almost anywhere and can transmit data in real-time. The goggle was developed by Dr. Liu Yang at the University of Akron in Ohio. The device is under US/Patent Cooperation Treaty (PCT) patent-protection (2, 3). Dr. Liu's initial focus was on clinical applications such as guiding cancer surgeries with the use of a goggle device. The device described here was derived from that original concept, but the new device required significant new capabilities. This report describes development of the new goggle device and its initial characterization.

The goggle prototype developed for real-time detection and identification of pathogens incorporates stereoscopic fluorescence imaging with a SmartGoggle Software. The prototype also can transmit captured images and video-recordings back to a computer for further data processing. Current technologies that the goggle prototype can compete with, such as the BioFire FilmArray and Biomeme two3 devices, use real-time PCR. However, real-time PCR out in the field has some cumbersome disadvantages in terms of requiring different reagents centrifuges, refrigerators, and freezers. The goggle device will not require extensive additional equipment and reagents.

The overall focus of the work done at CAMD was to test and evaluate the fluorescence detection capability of the goggle that Dr. Liu's lab developed at the University of Akron. An *in vitro* experimental strategy was devised to simulate fluorescence-based detection of the MERS-CoV spike protein. The approach used both polyclonal and monoclonal antibodies coupled to Alexa Fluor® 647, a red fluorescence dye with emission $\lambda_{max}$ at 647 nm. Three different purified forms of the spike protein were obtained from commercial sources, as were several monoclonal and polyclonal anti-spike protein antibodies. Two assay approaches were employed, one was the standard enzyme-linked immunosorbent assay (ELISA) and the other fluorescence-linked immunosorbent assay (FLISA). The readings were taken with the goggle and a benchtop 96-well plate reader.

We selected the MERS-CoV spike protein as the simulated target for detection because this Coronavirus, which emerged recently (2012), had a mortality rate of nearly 40 %, and therefore posed a particular regional threat, although at that time its pandemic potential could not be ruled out either (4). Unlike the MERS-CoV, four seasonal Coronaviruses are quite common – 229E, OC43, NL63, and HKU-1, but they do not raise any concerns, as they are relatively benign. Prior to emergence of the MERS-CoV in 2012, another deadly Coronavirus had emerged in China in 2002. Called the severe acute respiratory syndrome Coronavirus (SARS-CoV), this virus had a mortality rate of about 9.6 % (5). However, SARS-CoV remained largely restricted to China and some neighboring areas, and therefore did not become a global threat.

The emergence of the SARS-CoV-2 in Wuhan, China in December 2019 presents itself as a fundamentally different case of deadly viral outbreak and spread. Within weeks of the first reported cases in December 2019, the virus had become pandemic. As of 5 August 2020 there were over 18 million worldwide cases, with over 700,000 deaths. In the United States the outbreak was particularly severe, with over 4.8 million cases and 157,000 deaths (6). Although not the subject of this study, we note these data to signify the need for light, portable, highly sensitive pathogen detection devices that could be deployed on short notice in areas of pathogen emergence (7). The goggle developed in this study is one such candidate instrument.

## MATERIALS AND METHODS

### The goggle prototype for pathogen screening

The prototypic goggle was developed in Dr. Liu's laboratory at the University of Akron, Akron, Ohio. Several different components and aspects had to be developed. These included imaging, illumination, display, analysis, and control modules. The various modules were integrated to assemble the functional goggle prototype. A special software package was also developed for the goggle (Figures 1 and 2).


**Figure 1. Front view of the fluorescence-detecting pathogen-screening goggle**.

**Figure 2. Inside view of the fluorescence-detecting pathogen-screening goggle**.

**Goggle display controller**

When wearing the goggle prototype, the Display Controller, shown in Figure 3, is used to help display an image on the goggle device so that a user can see the image or the field of view in real-time. The user can adjust the brightness and contrast up or down by pressing the plus (+) or minus (-) buttons.


**Figure 3. The goggle display controller box**.

**The stand-mounted light source for excitation of the fluorescent dye Alexa Fluor® 647**

Components of the stand-mounted device for detection of Alexa Fluor® 647 fluorescence are described below (Figures 4 - 6).

**Figure 4. Stand-mounted light source for excitation of the fluorescent dye Alexa Fluor® 647**.


**Figure 5. Back view of the stand-mounted light source for Alexa Fluor® 647 excitation**.

**Figure 6**. **Front view of the stand-mounted light source for Alexa Fluor® 647 excitation**. The source is directly positioned over the experimental vial in which the specific-pathogen detection biochemical interactions result in emission of fluorescence, e.g., for specific detection of MERS-CoV spike protein. For the work described in this report, the detection wavelength was set at 647 nm in the red range of the visible light spectrum.

**<u>The hand-held Alexa Fluor® 647 excitation light source</u>**

Initial testing of the goggle prototype was done using the stand-mounted excitation source. However, due to the 96-well plate format, the hand-held excitation light source, shown in Figure 7, was a better option. The hand-held light source is set for Alexa Fluor® 647 and has a higher intensity when compared to the stand-mounted version. This smaller version has 5 modes (very low, low, medium, high, and ultra-high), and the user can switch from mode to mode by pressing the silver colored button on the side of the light source.


**Figure 7. A side view of the hand-held light source set at the excitation wavelength for Alexa Fluor® 647**.

**Goggle computer**

The computer is an Intel NUC mini PC with Ubuntu 16.04 operating system, shown in Figure 8. The goggle computer system includes monitor, keyboard, and mouse.

**Figure 8. Intel NUC mini PC**.

**SmartGoggle Software**

SmartGoggle software (version 3.0) was preloaded on the mini-PC and was accessible through a shortcut on the desktop. The SmartGoggle software provided graphical user interface (GUI) to set file-save path, camera parameters, and various other software parameters. The ImageJ software (version 1.52a) was used to visualize and quantify band intensity.

**Detection of MERS-CoV spike proteins with monoclonal and polyclonal antibodies**

Black 96-Well ELISA plates (Nunc; ThermoFisher, cat. # 437111) were coated overnight with different MERS-CoV spike proteins at various concentrations in 100 µL of phosphate buffered saline (PBS) or carbonate-bicarbonate buffer. The plates were washed 3 times with 300 µL of PBS-Tween 20 and then blocked with 300 µL of 1x Blocker BSA (ThermoFisher, cat. # 37525) for 3 hours at room temperature. After that, the plates were washed 3 times with 300 µL of PBS-Tween 20. Various concentrations of monoclonal or polyclonal antibodies were added, followed by incubation at 37$^{o}$C for 1 hour. The plates were washed as before. Alexa Fluor® 647 Goat anti-mouse antibodies (Abcam, cat. # ab150115) or Alexa Fluor® 647 goat anti-rabbit antibodies (Abcam, cat. # ab150099) were added to the plates, followed by further incubation at 37$^{o}$C for 1 hour. The plates were washed again as described above. Fluorescence emission was measured with BioTek Synergy H1 plate reader. The excitation wavelength was 638 nm and the emission wavelength 668 nm.

**Fluorescence-linked immunosorbent assay for detection of MERS-CoV**

The procedure for the fluorescence-linked immunosorbent assay (FLISA) was like the procedure as described under the “detection of MERS-CoV spike proteins with monoclonal and polyclonal

antibodies" above. The main difference is that in the FLISA the plates were first coated with capturing monoclonal antibodies overnight at 4$^{o}$C. The next day the plates were washed to remove free antibodies, followed by blocking with BSA overnight at 4$^{o}$C. Next, the plates were washed to remove free BSA, different concentrations of spike proteins added, and the plates incubated at 37$^{o}$C for 1 hour. The plates were then washed with PBS-Tween 20 before addition of the detecting polyclonal antibodies. The plates were incubated at 37$^{o}$C for 1 hour and then washed. The Alexa Fluor® 647 goat anti-rabbit antibodies were added for the fluorescent detection with the BioTek Synergy H1 plate reader.

## RESULTS

### Development and testing of imaging module

We have developed an imaging module for the fluorescence-sensing prototype goggle, with the long-term aim to make it deployable for fast detection of high priority pathogens. A device with small form factor and light weight enhances integration and makes the goggle easy to wear. Additionally, low dark noise level and high quantum efficiency and resolution are required for high sensitivity in low-light environments. To this end, we have selected 2 imaging sensors for continued development: the Sony ICX818 CCD sensor and the e2v EV76C661 CMOS sensor. The Sony ICX818 sensor was selected for its lower dark noise, an advantage of CCD technology. We have characterized the ICX818 for fluorescence detection limits and spatial resolution (Figures 9A-C). The e2v EV76C661 provides an alternative sensor which benefits from enhanced quantum efficiency and a faster frame rate. Another benefit of both sensors is lower power consumption, owing to their small integrated circuit boards which do not require external cooling systems. This makes both devices suitable for systems that may need to run on battery for a long time.

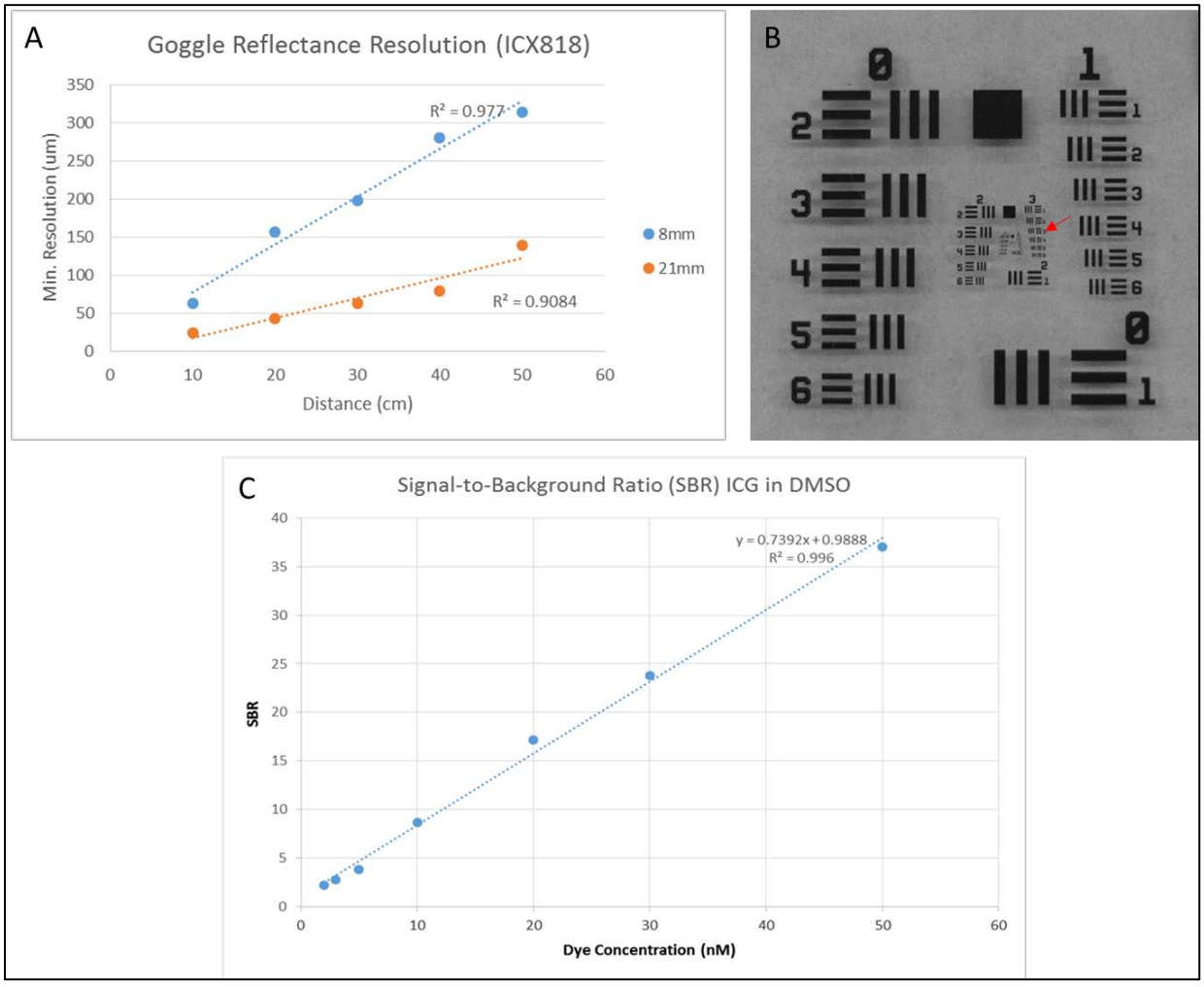

**Figure 9. A,** Reflectance mode spatial resolution of the Sony ICX818 imaging module using an 8 mm and 12 mm lensing system. The resolution is linear across various working distances. With a minimum resolvable object size of less than 50 µm. **B,** USAF bar pattern imaged by the Sony ICX818 with the 21 mm lens. The red arrow indicates the minimum resolvable pattern visible to the human eye. **C,** Fluorescence detection limits for the imaging module of a near-infrared fluorophore (ICG). The minimum detectable concentration of ICG, defined as having a signal-to-background ratio (SBR) of 2, is 2.5 nM. The SBR increases linearly with dye concentration.

We have continued the characterization of our imaging module sensors by conducting resolution and fluorescence detection sensitivity testing of the e2v EV76C661 CMOS sensor. The enhanced quantum efficiency of the e2v EV76C661 was demonstrated to provide greater sensitivity to near-infrared (NIR) fluorescent emissions than our other imaging sensor, the Sony ICX818 (Figure 10C). Using a signal-to-background ratio (SBR) of 2 as a minimum detection level, we have determined that the e2v sensor can detect NIR emissions down to a concentration of 300 pM. The ICX818 can detect fluorescent emissions down to a concentration of 3 nM. The resolution of the e2v sensor is less than that of the ICX818 (Figures 10A-10C).

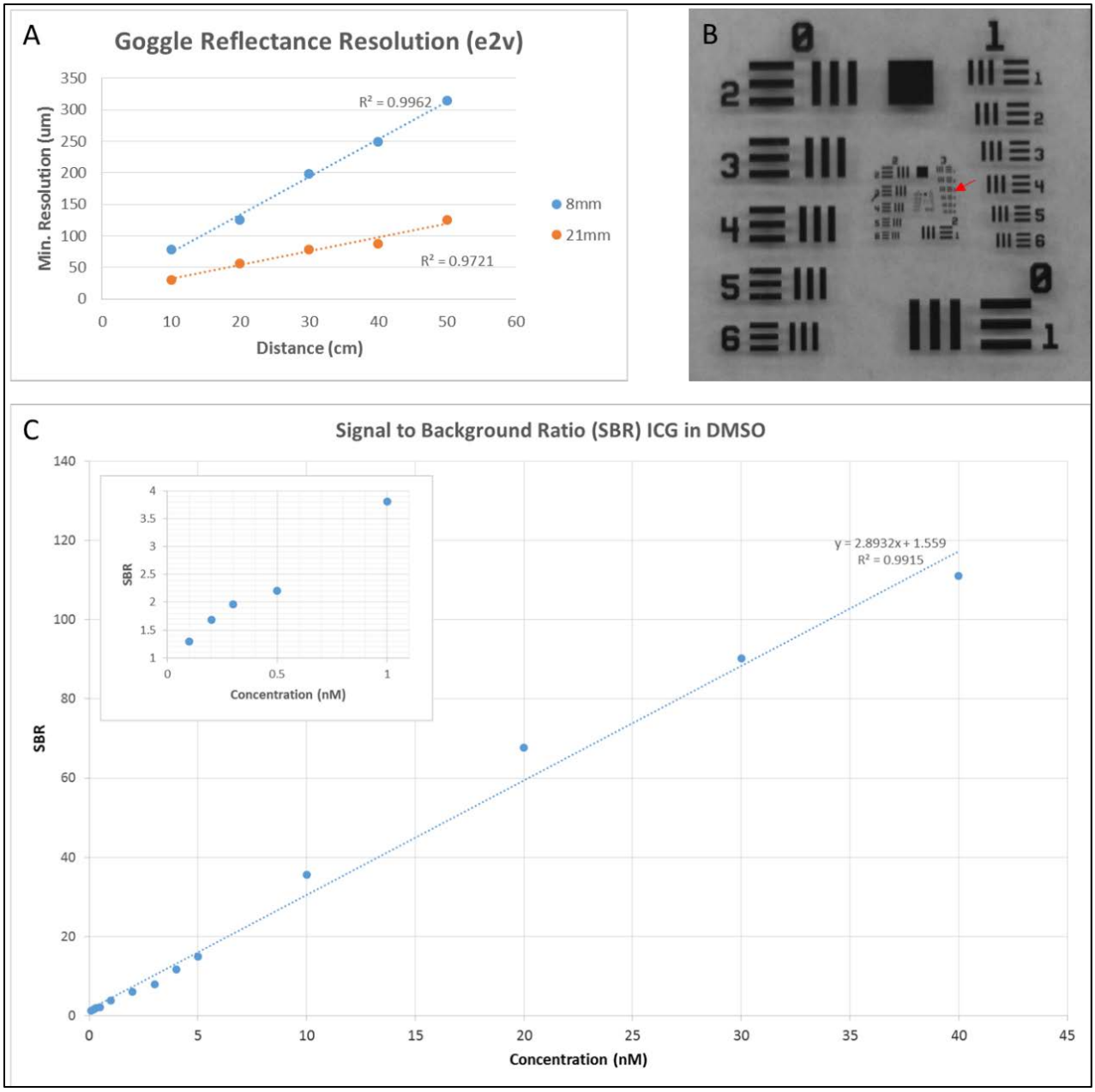


**Figure 10. A,** Reflectance mode spatial resolution of the e2v EV76C661 imaging module using an 8 mm and 21 mm lensing system. The resolution is linear across various working distances. With a minimum resolvable object size of less than 50 µm. **B,** USAF bar pattern imaged by the Sony ICX818 with the 21 mm lens. The red arrow indicates the minimum resolvable pattern visible to the human eye. **C,** Fluorescence detection limits for the imaging module of a near-infrared fluorophore (ICG). The minimum detectable concentration of ICG, defined as having a signal-to-background ratio (SBR) of 2, is 0.3 nM. The SBR increases linearly with dye concentration. **Inset in C,** A detailed depiction of SBR vs. concentration data in the 0.1 to 1 nM ICG concentration range.

**Development of the illumination module**

We have continued to refine our prototype illumination module for the goggle system, as shown in Figure 11A. The new prototype illumination module utilizes high power LEDs and provides for a cooled, high output, stable, variable intensity illumination source with a small form factor which is easy to transport, set up, and use. The illumination region is well-defined and uniform, which can be conveniently expanded or shrunk to meet the user needs. The new design incorporates 2 subunits, one for fluorescence excitation and one for broad spectrum illumination.

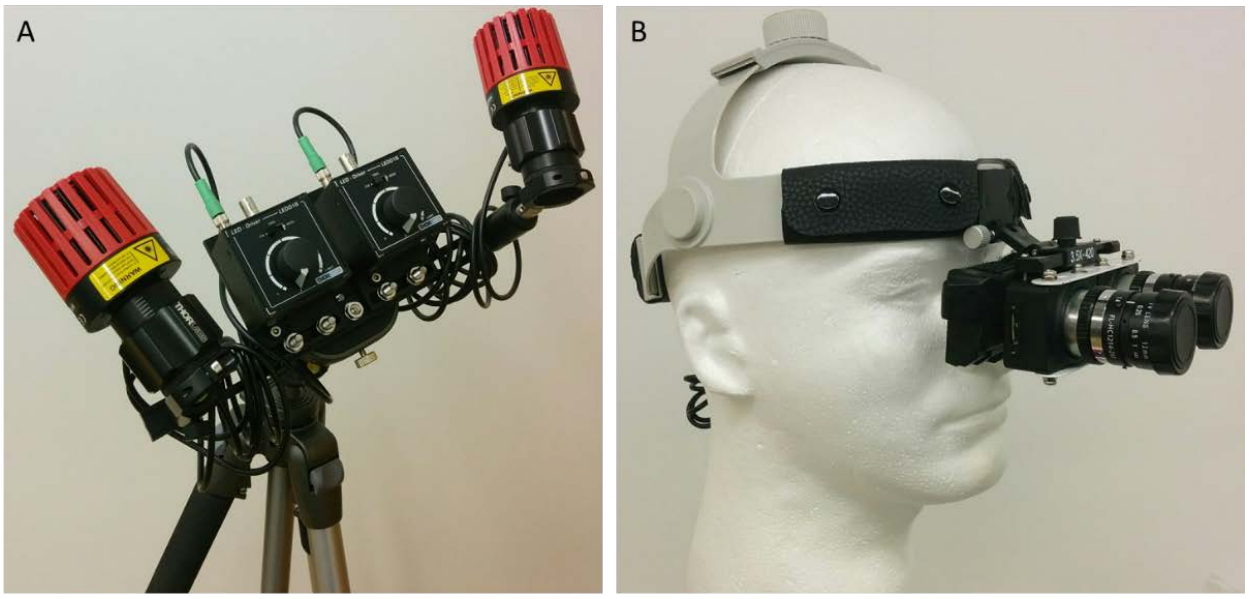


**Figure 11. A,** New prototype illumination module with dual adjustable subunits (red). **B,** Integrated imaging, and display module connected to an adjustable head-mount.

Based on the feedback from CAMD, a prototype handheld light source was developed, as shown in Figure 12. This handheld light source is compact and battery-operated. It offers 3 levels of excitation intensities controlled by push buttons. The light source is convenient to transport (total weight ~ 160 g), and can be used with ease. The handheld light source implementation better simulates the battlefield situation and will pave the way for field-deployable systems in the future.

**Figure 12. Compact hand-held light source for fluorescence excitation. The light source is battery-operated and easy to carry**.

**The display modules**

Owing to small form factor, light weight, ease of integration, strong optical performance, and availability we have tailored our display module based on the liquid crystal display (LCD) technology in the transmissive geometry for our prototype system. The display module has been integrated with the Sony ICX818 imaging module to create a prototype wearable imaging goggle. In comparison to other small form factor display technologies that use liquid crystal technology on silicon (LCoS) or projection, the current display module was developed to have superior optical quality and visual clarity. We note here that we have also investigated integrating some existing technologies, such as Oculus, HTC Hive, and Hololens, as the display module. However, we determined that such display modules have larger form factors, which would increase the overall footprint of the systems, and therefore would be less desirable for portability.

**The Control modules**

All system components including the imaging, illumination and display modules are integrated into an Intel NUC small computer and controlled through custom software we developed. Owing to its ease of use and quick trouble-shooting capability, the Python language was used to develop the software. The software allows the user to activate or deactivate each connected module, while reading, processing, saving, and displaying active data in real-time. The control module also integrates imaging data into the head-mounted display unit while duplicating the display on the PC monitor.

**Prototype goggle for specific detection of Alexa Fluor® 647 fluorescence**

Alexa Fluor® 647 is a red fluorescence dye commonly used for labeling proteins. The biochemical assay used at CAMD for detection of the MERS-CoV spike protein employed this dye. For the work reported here, therefore, we adapted the prototype goggle for specific detection of fluorescence from this dye.

To test the system performance, we made various dilutions of Alexa Fluor® 647 in DMSO. The final dye concentrations were 500, 250, 100, 75, 50, 25, 10, 7.5, 5, 2.5, 1, 0.75, 0.5, and 0.25 nM. Different concentrations of the fluorophore were tested under three different illumination intensities: 25, 200, and 300 µW. The illumination spot intensity was measured by ThorLabs PM160 light meter.

The detection limits of the system for Alexa Fluor® 647 was characterized (Table 1). The results show that at 300 µW illumination and signal-to-background ratio of 1.2, the system can detect fluorescence signal down to 0.5 nM concentration of the dye.

**Table 1**. The lowest detected Alexa Fluor® 647 concentrations with a signal-to-background ratio (SBR) of 1.2 or 2 at various illumination intensities (Power).

| SBR | Test # | Minimum detected conc. (nM) | Power (µW) |
|---|---|---|---|
| 1.2 | 1 | *5.6* | 25 |
| | 2 | *0.7* | 200 |
| | 3 | 0.5 | 300 |
| | | | |
| 2 | 1 | *33* | 25 |
| | 2 | *3.3* | 200 |
| | 3 | *1.8* | 300 |

Italicized numbers, interpolated

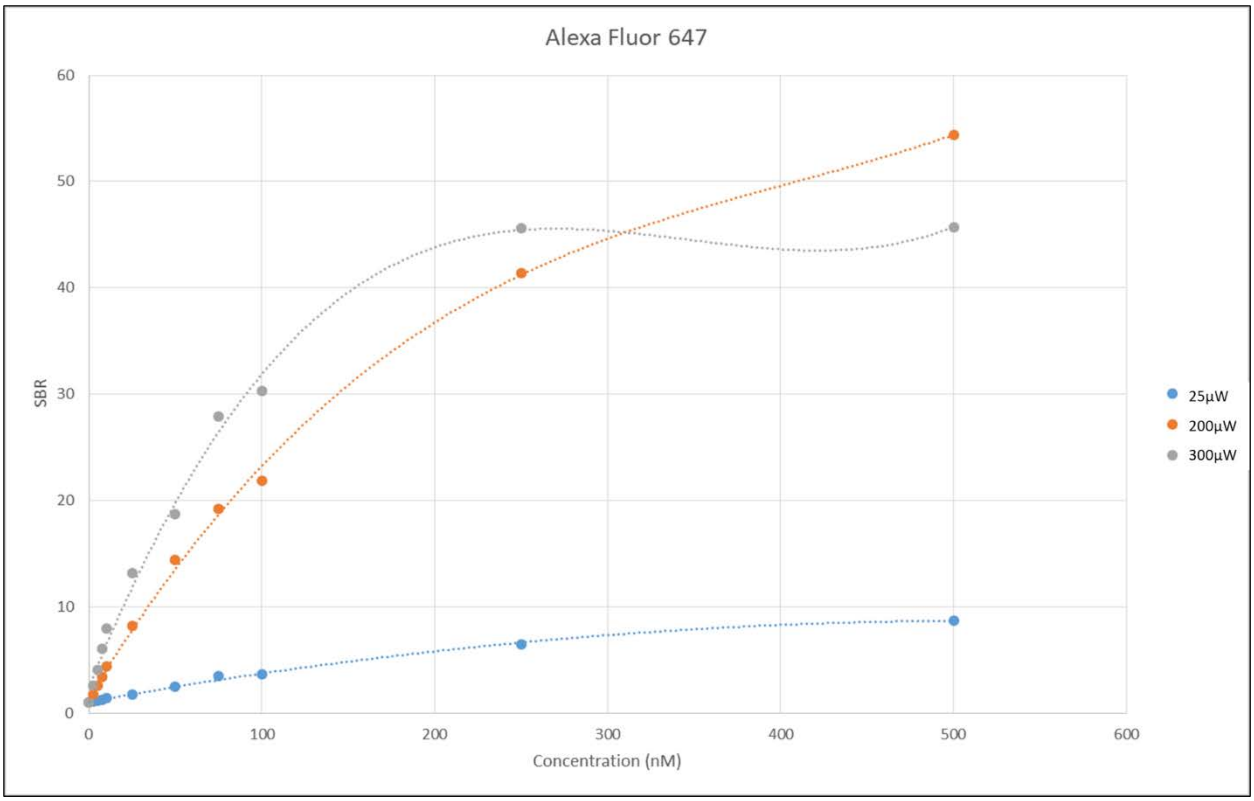


**Figure 13. Signal-to-background ratio (SBR) of dilution series for various illumination intensities**. Trendlines are 2nd order polynomials. Large SBR are found across the dynamic range of Alexa Fluor® 647 concentrations.

A representative image of dilutions from 2.5 to 500 nM under 200 µW illumination is shown in Figure 14. Note that the goggle can accommodate a wide range of concentrations of Alexa Fluor® 647 and offer a wide dynamic range.


**Figure 14. An image of various dilutions of Alexa Fluor® 647 detected with the fluorescence-sensitive goggle at 200 µW illumination**. The dye dilutions were 50, 75, 100, 250, and 500 nM.

**Development of a user-friendly software package**

The software package developed is in the Python coding language. The package has multiple components which can be operated independently or in conjunction with one another. The goggle script runs the Multipurpose Imaging Goggle, capturing and processing images and displaying them both on the connected PC and the goggle display module. Dividing the code into integrable but independent components affords the user the ability to use each part of the system together, but also singly.

We have optimized the software package to improve its functionality and user-friendliness. Currently, the PC connected to the goggle runs Ubuntu 16.04 operating system. The current version (2.1) of the goggle software (*SmartGoggle application*) is pre-loaded and accessible through a shortcut on the desktop (Figure 15).


**Figure 15. SmartGoggle application is readily accessible from the desktop shortcut**.

SmartGoggle application provides Graphical User Interface (GUI) that is used to set file save path, camera parameters, and different other control levels of the application. Some of these parameters and options are briefly described below and shown in Figure 16.

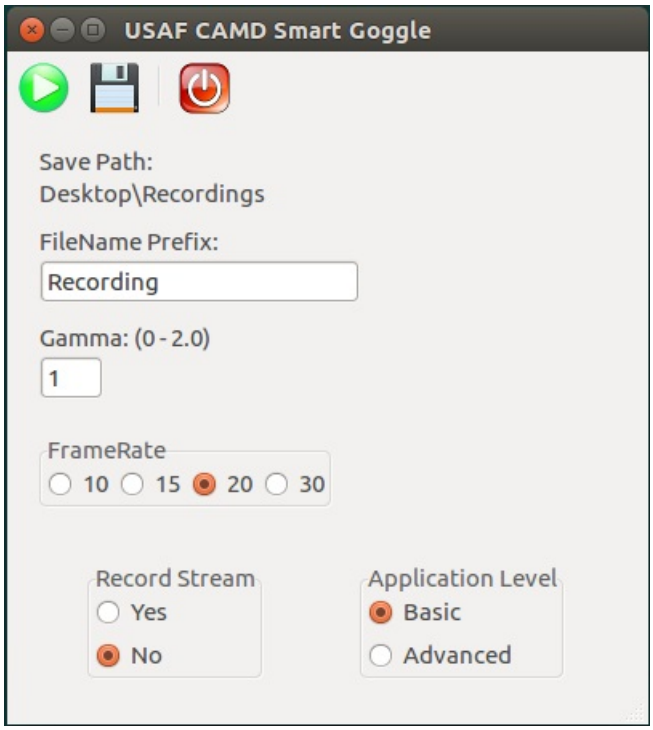


**Figure 16. A screen-shot image of the SmartGoggle application GUI**.

**Select file save path:** The diskette icon shown in Figure 16 allows user to change the file save path when the video file or a single image is being saved. The image files or the video files will be saved under the designated file save path (e.g., C:\GoggleDataCAMD\). Save path shows the default directory for recorded video and image files. Changes will be shown as "New Path" on a new line.

**FileName Prefix:** This allows user to choose a certain prefix for each set of videos and image files, to make file management more convenient. Each recorded file is uniquely named starting with the prefix followed by the current date and time. For example, if the user designates FileName Prefix as "CAMD," and the date is 7 June 2020, the file name will be in this format: CAMD_20200610_1239.avi.

**Gamma:** This option allows user to change the gamma setting for output images. This value will be implemented directly on raw camera output images and videos. Inputs can be any float-point number from 0 to 2.

**FrameRate:** With this option the user can manually set the working frame rate of cameras. Frame rate is the rate at which consecutive images, called frames, appear on a display in a video file, expressed as per second, e.g., 30 frames per second (fps). Changing the frame rate changes the ceiling for sensor exposure time. This means the lower the frame rate, the longer the imaging sensors' exposure to light, which would result in brighter video outputs. However, one drawback for an extremely low frame rate (e.g., < 10 fps) might be that the videos could become choppy. Imaging sensors' gain and exposure time are therefore automatically adjusted for the best contrast and brightness, based on the frame rate designated by the user.

**Record Stream:** This option allows the user to choose whether to save the video stream as a file. To save the video stream, the file path shown as "Save Path" or "New Path" selected by user will be used as the target folder. The output will be saved as ".avi" file, which can then be played on most commercially available video players (e.g., VLC media player, windows media player).

**Application mode:** The application has two modes, Basic and Advanced. The Basic mode is for the raw output images. The Advanced mode runs multiple image processing functions, including brightness adjustment and color mapping with threshold adjustment. By changing the threshold, higher contrast can be achieved for easier visualization.

**Hotkeys:** The following hotkeys are available in the Advanced mode and pressing one of these keys while the Goggle is running will result in the effect that corresponds to that key's functionality.

**A:** Increase Brightness

**B:** Decrease Brightness

**T:** Activate/Deactivate ColorMap

**S:** Save an image

**D:** Increase Threshold Level

**C:** Decrease Threshold Level (lower lights will be considered as fluorescence)

**Q:** Quit Program (Q works on both *Advanced* and *Basic* modes)

## System testing and characterization

Two imaging modules have been tested, the e2v EV76C661 CMOS sensor and the Sony ICV818 CCD sensor. Near-Infrared (NIR) fluorescent emissions down to a concentration of 300 pM were detectable on a dark background by the e2v sensor (Figure 17A). The Sony sensor detected fluorescent emissions down to a concentration of 3 nM. The resolution of the Sony sensor is greater than that of the e2v, with slightly lower salt & pepper noise (Figure 17B). Imaging resolution, fluorescence detection limits, ease of integration, and user compliance all factored into sensor selection.

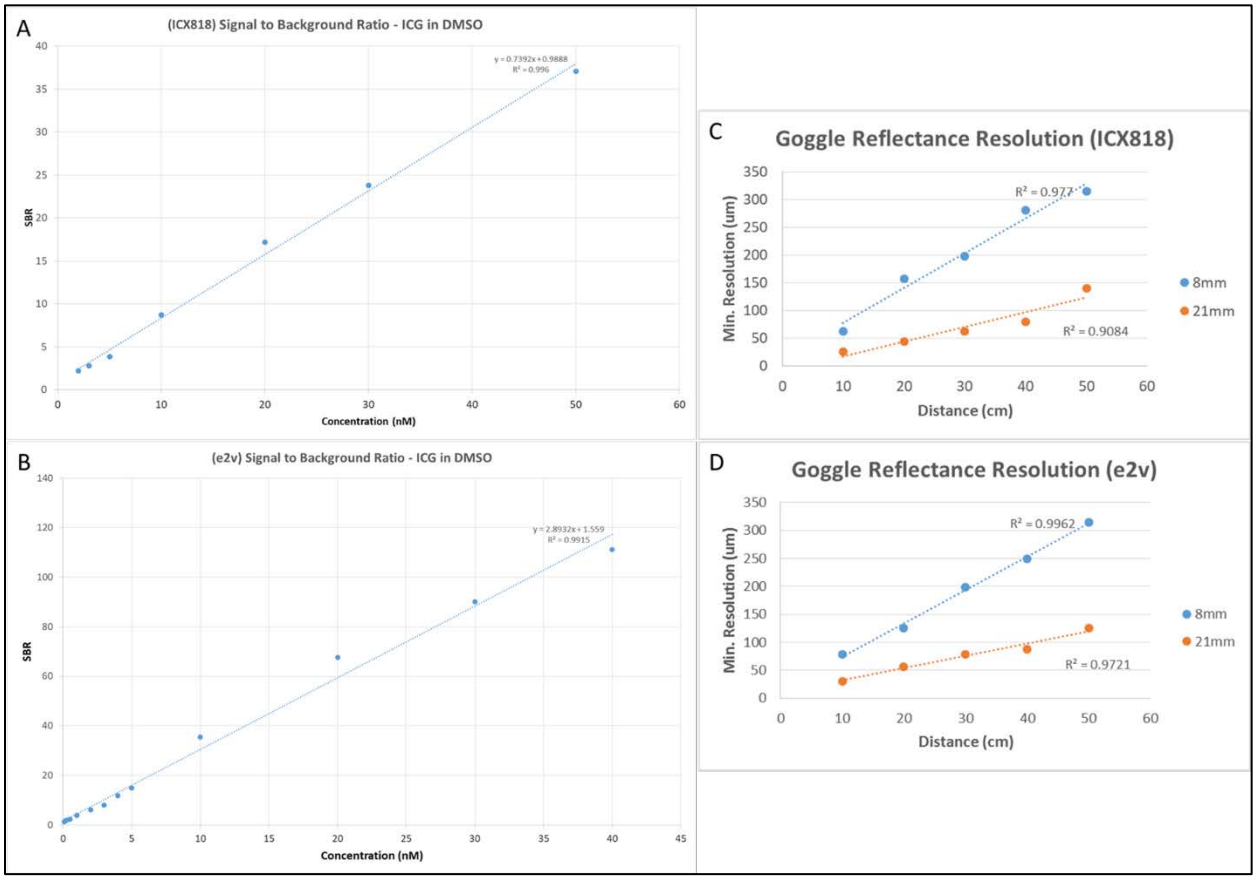


**Figures 17**. Signal-to-background ratio NIR fluorescence detection by the Sony CCD (**A**) and e2v CMOS (**B**) imaging sensors. **C & D,** Imaging sensor resolution for the Sony CCD (**C**) and e2v CMOS (**D**) sensors using both 8 mm and 21 mm lenses at various working distances.

We have further characterized the prototype systems for Alexa Fluor® 647 in terms of parameters such as signal-to-background ratio at 300 µW illumination. These data are shown in Figure 18.

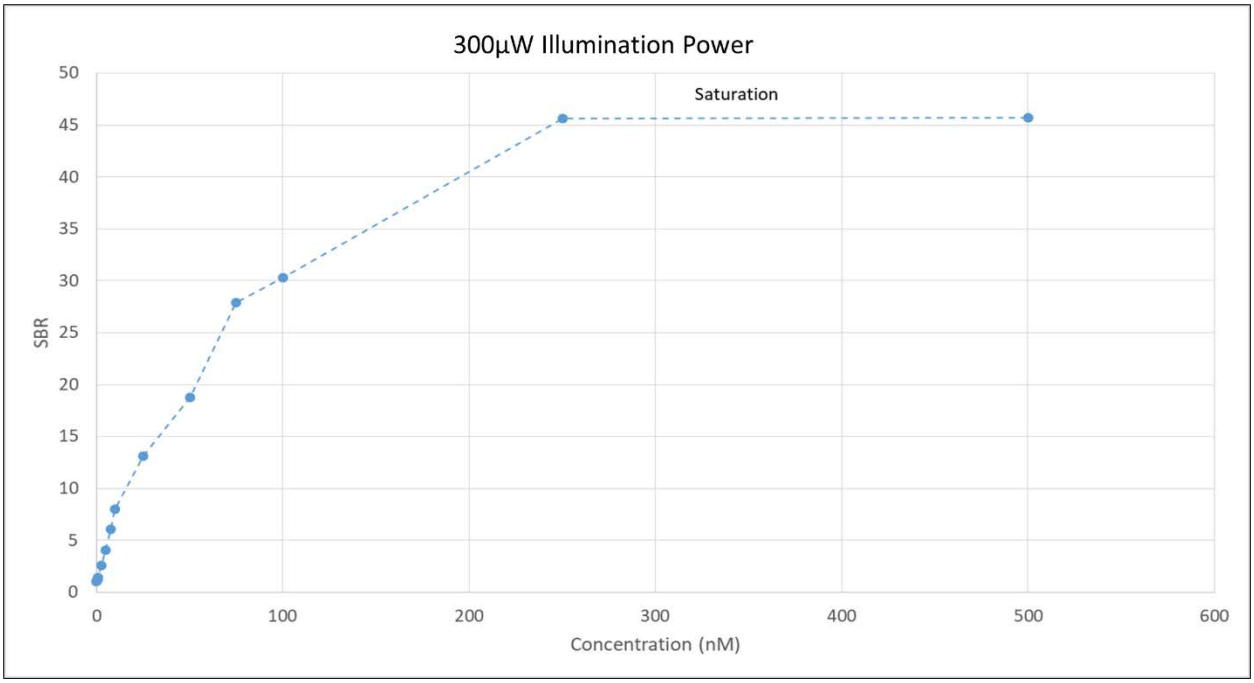


**Figure 18. SBR of dilution series at 300 µW illumination intensity**. Under these conditions, the SBR maximum occurred at about 250 nM concentration of Alexa Fluor® 647 and then leveled off. The minimum detectable concentration for SBR = 1.2 is 0.5 nM.

We have found that minimum fluorescence detection with room lights on, illumination intensity at 300 µW, and SBR at 1.2 was about 5 nM. A representative data of 5 nM is shown in Figure 19.

**Figure 19.** The minimum Alexa Fluor® 647 fluorescence detection with room lights on, with illumination intensity set at 300 µW and SBR = 1.2. The minimum was found to be about 5 nM. The left vial is control (no fluorophore) and the right vial contains Alexa Fluor® 647 at 5 nM concentration.

We have further designed another test using droplets to characterize the prototype system. The findings showed the high detection sensitivity of the prototype (Figure 20).

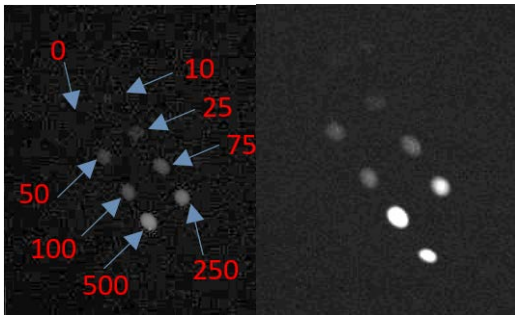


**Figure 20. 1-µL droplets of approximately 2 mm diameter imaged under 300 µW illumination intensity**. In this experiment, the 10-nM Alexa Fluor® 647 drop was the lowest concentration detectable with an SBR of at least 1.2. Notice, however, that in this picture the 10-nM drop is not readily visible; the 25-nM drop is the lowest readily visible drop. Further, the droplets down to 0.25 µL and 0.5 mm diameter were imaged at a concentration of 25 nM as well.

**Evaluating the Multipurpose Imaging Goggle**

We have evaluated the Multipurpose Imaging Goggle with Alexa Fluor® 647, in terms of fluorescence imaging resolution, to characterize its ability for infectious disease threat identification and surveillance.

To evaluate realistic scenario that simulates in-field surveillance application, we sprayed a solution of Alexa Fluor® 647 dissolved in DI water onto a glass USAF 1951 Resolution Target, which was placed upon a white glazed ceramic tile. The fluorescence was excited with the custom light source comprising of a 660 nm LED emitter equipped with a 650 nm short pass filter. Imaging was conducted via the goggle prototype having a band pass filtered for AF 647 with a central wavelength of 671 nm, at working distances of 20, 40, and 60 nm. Imaging was conducted in a dark room using either the excitation LED for fluorescence detection or a white light LED for reflectance imaging.

The fluorescence images were processed using a binary threshold operation and false colored to make the droplets more apparent. The white light images of the resolution target and the fluorescence images of the droplets were then combined using a direct addition (Figures 21-26).

Comparing the sizes of the smallest visible fluorescence emitting droplets to the widths of the various bar patterns allows us to evaluate the fluorescence resolution of the system. The goggle can detect AF 647 down to a 99 µm resolution.

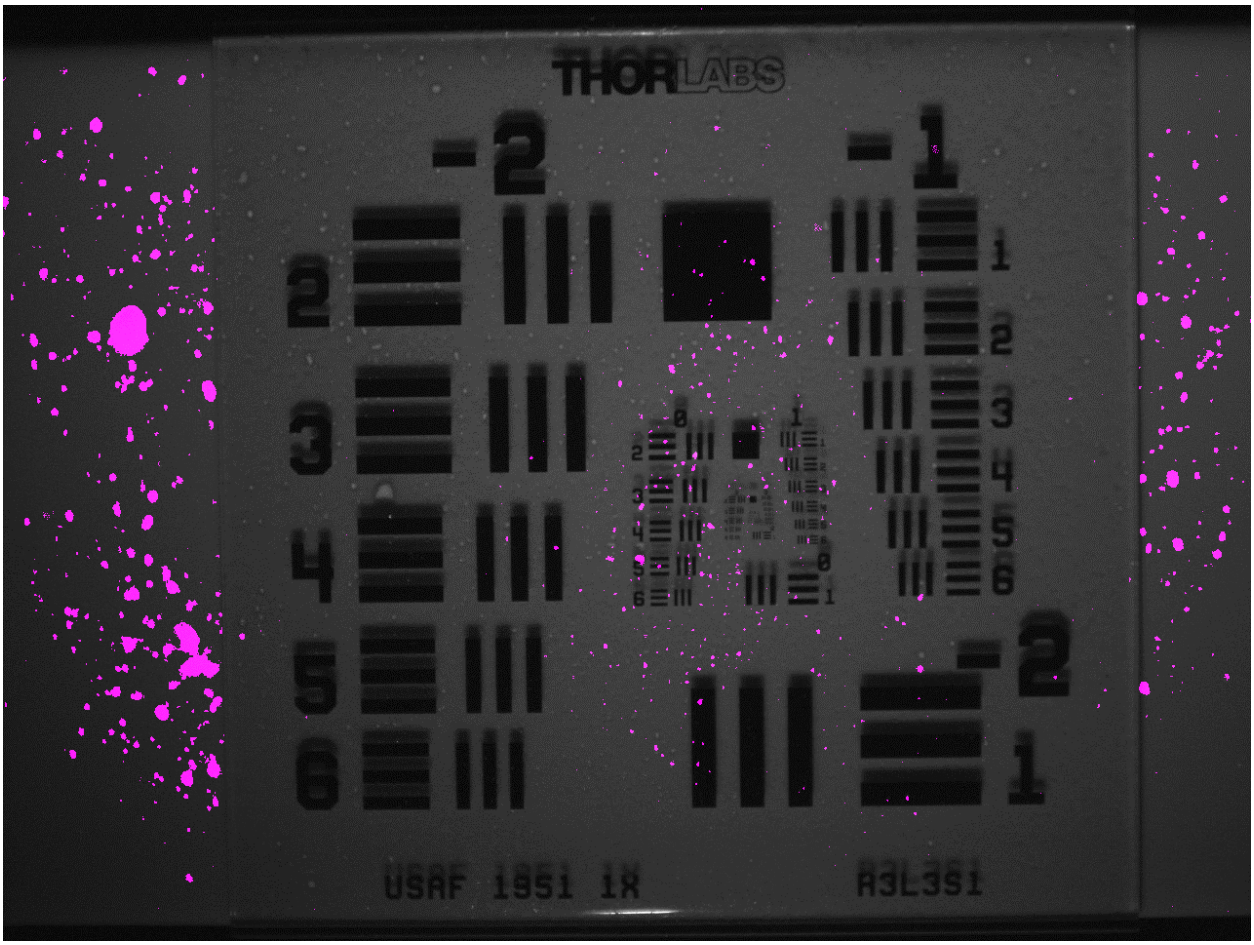


**Figure 21**. **USAF 1951 Resolution Target with fluorescent droplets of the AF 647 Alexa Fluor® 647 solution in magenta**. Image taken at a 20 cm working distance from target to the goggle.

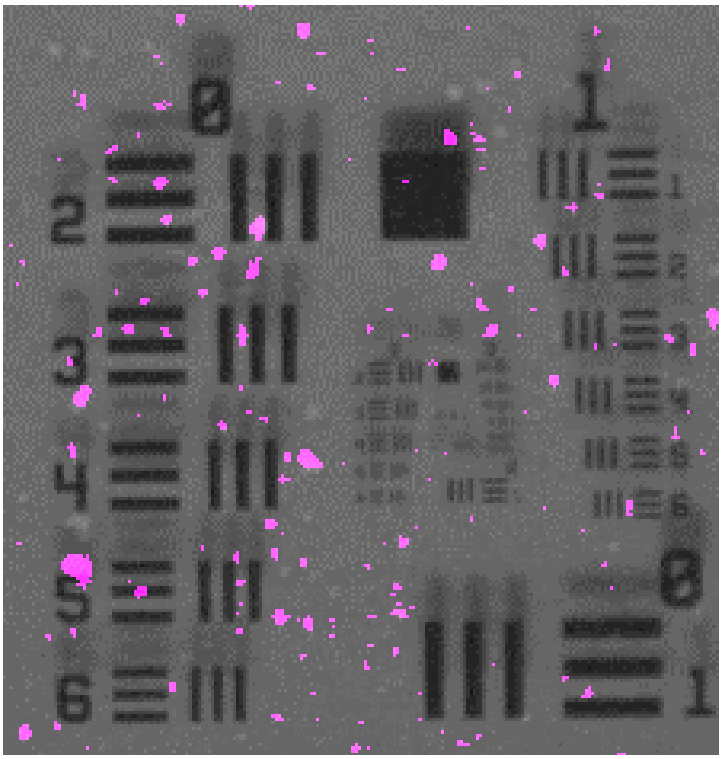

**Figure 22. Enlarged view of the central set of bar patterns taken from Figure 21**. The image has been digitally brightened to make the bars more visible.

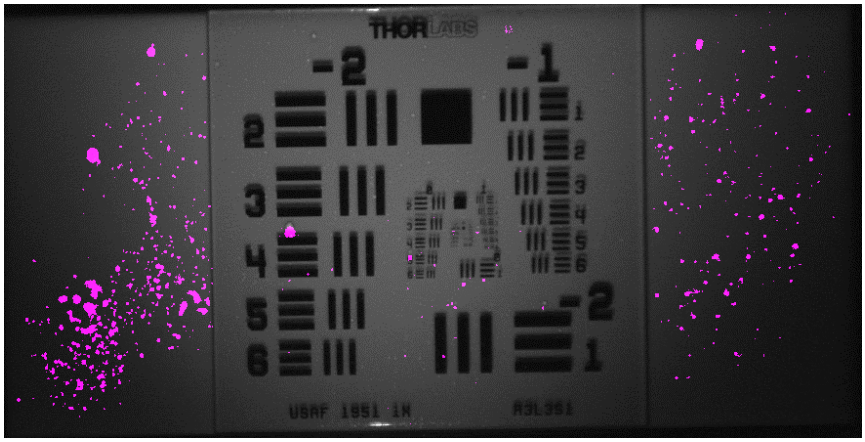


**Figure 23. USAF 1951 Resolution Target with fluorescent droplets of the Alexa Fluor® 647 solution in magenta**. Image taken at a 40 cm working distance from target to the goggle.

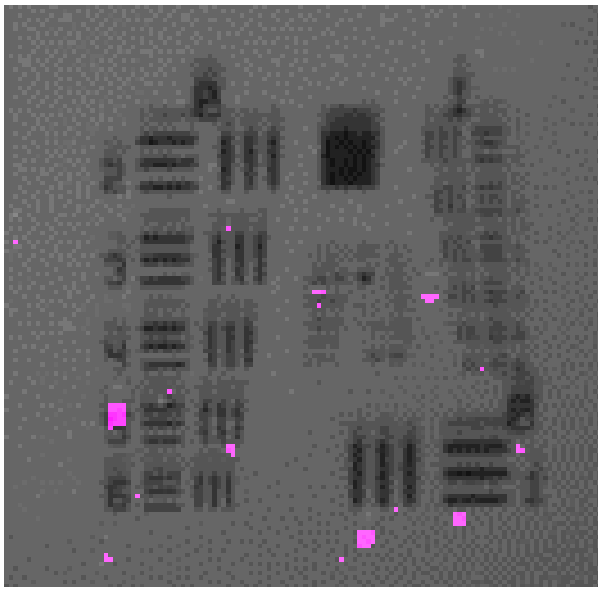

**Figure 24. Enlarged view of the central set of bar patterns taken from Figure 21**. The image has been digitally brightened to make the bars more visible.

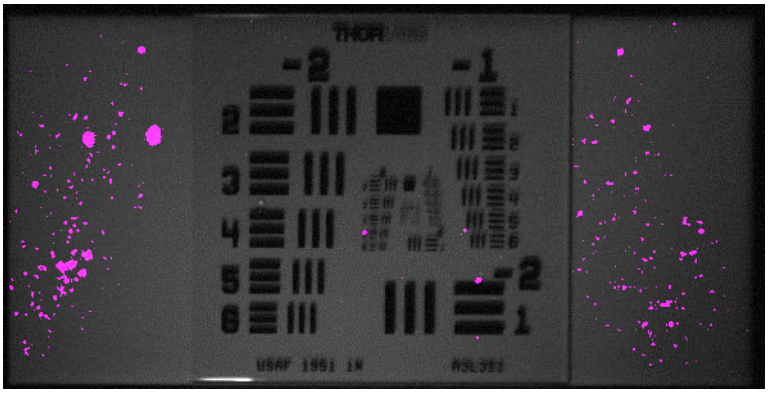


**Figure 25. USAF 1951 Resolution Target with fluorescent droplets of the AF 647 Alexa Fluor® 647 solution in magenta**. Image taken at a 60 cm working distance from target to goggle camera.

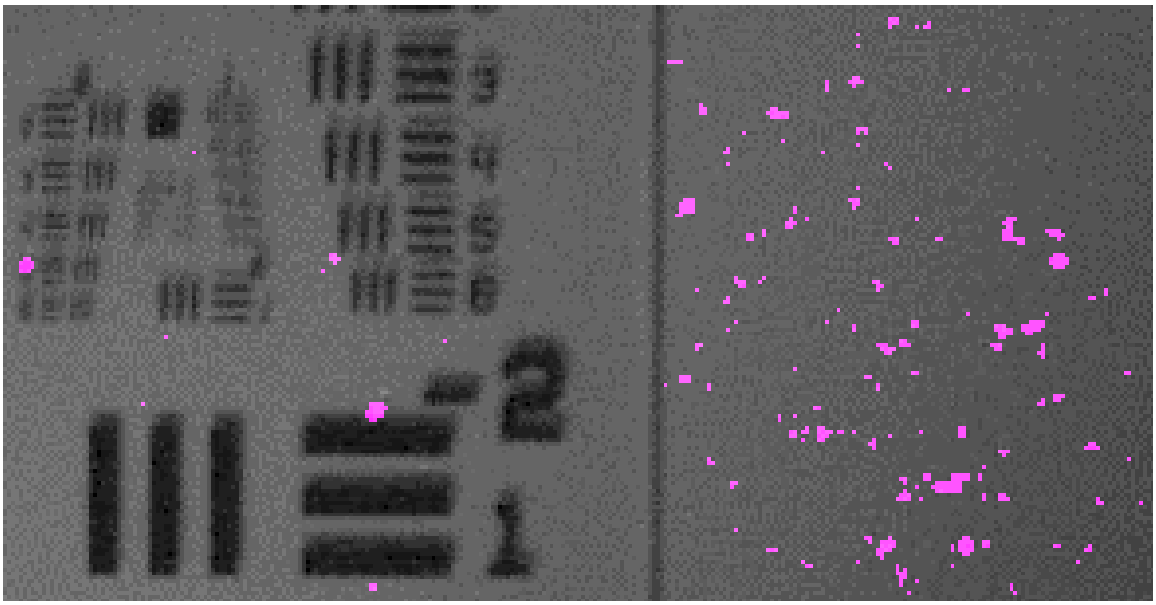

**Figure 26. Enlarged view of the central set of bar patterns taken from Figure 25**. The image has been digitally brightened to make the bars more visible. Part of the ceramic tile was included in this crop to include more droplets for size comparison.

**Table 2. The goggle reflectance and fluorescence measurements in relation to working distance.**

| Working Distance (cm) | Fluorescence Resolution (µm) | Reflectance Resolution (µm) |
|---|---|---|
| **20** | 99 | 88 |
| **40** | 157 | 140 |
| **60** | 280 | 250 |

Reflectance resolution refers to the smallest visibly distinguishable set of horizontal and vertical bars. Higher resolutions are likely also achievable under brighter illuminations (room lighting) and with the fluorescence emission bandpass filter off the camera lens. However, the effort here was to replicate realistic working conditions for in-field surveillance. Threshold levels and droplet sizes were determined following 3 trials, with averaging of multiple droplet measurements within each trial.

**Fluorescence-linked immunosorbent assay (FLISA) for the detection of MERS-CoV spike protein**

The *in vitro* fluorescence-based assay for the detection of MERS-CoV spike protein was used at the Center for Advanced Molecular Detection (CAMD) to test the fluorescence detection capability of the goggle prototype. We conducted screening to identify the best antibody-antigen combinations for the detection of MERS-CoV spike protein using the FLISA method. The best combination was using the mAb 1 as the capturing antibody, the pAb3 as the detecting antibody,

and the spike protein 1 as the target (Table 3). The Alexa Fluor® 647 goat anti-rabbit IgG was used to detect the pAb and to provide the fluorescence signal.

**Table 3. Antibodies and MERS-CoV spike proteins used in this work for FLISA**.

| Assigned Name | Reagent Name, vendor, catalog number |
|---|---|
| Spike protein 1 | MERS-CoV spike S1 protein, eEnzyme, MERS-S1-005P[1] |
| Spike protein 2 | MERS-CoV spike S1 protein, MyBioSource, MBS430257[2] |
| Spike protein 3 | Receptor binding domain of MERS-CoV Spike Protein, eEnzyme, MERS-RBD-005P[3] |
| mAb 1 | Anti-S1 (MERS-CoV/HCoV-EMC/2012) monoclonal antibody, eEnzyme, MERS-S1-001[4] |
| mAb 2 | Anti-S1 (MERS-CoV/HCoV-EMC/2012) monoclonal antibody, MyBioSource, MBS430177[4] |
| mAb 3 | S1 (MERS-CoV/HCoV-EMC/2012) monoclonal antibody, MyBioSource, MBS430178[4] |
| pAb 1 | Anti-S1 (MERS-CoV) polyclonal antibody, eEnzyme, MERS-S1-015[5] |
| pAb 2 | Anti-MERS-CoV spike protein S1 (N-terminal) polyclonal antibody, Creative Diagnostics, CABT-B1954[6] |
| pAb 3 | Anti-MERS-CoV spike protein S1 (aa 1-725) polyclonal antibody, Creative Diagnostics, CABT-B1960[7] |

**Notes:**

1. **MERS-S1-005P** (eEnzyme) is the MERS-CoV S1 protein aa 1 – 725 with C-terminal 6x His tag. The sequence is based on the full-length, 1353 aa S1 protein of the human Betacoronavirus 2c Jordan-N3/2012, GenBank accession # AHY21469.1.
2. **MBS430257** (MyBioSource) is the MERS-CoV S1 protein aa 1 – 725 with C-terminal 6x His tag. The sequence is based on the full-length, 1353 aa S1 protein of the human Betacoronavirus 2c EMC/2012, GenBank accession # AFS88936.1. The Jordan-N3/2012 and the EMC/2012 full length S1 proteins differ at only two positions: at position 94, Jordan-N3/2012 has valine, EMC/2012 has glycine; at position 194, Jordan-N3/2012 has tyrosine, EMC/2012 has histidine.
3. **MERS-RBD-005P** (eEnzyme) is the MERS-CoV S1 protein segment termed the receptor-binding domain (RBD), aa 358 – 588, with C-terminal 6x His tag. The sequence is based on the full-length, 1353 aa S1 protein of the human Betacoronavirus 2c Jordan-N3/2012, GenBank accession # AHY21469.1. The RBD sequence of Jordan-N3/2012 and EMC/2012 viral isolates is identical.
4. **MERS-S1-001** (eEnzyme)**, MBS430177** (MyBioSource)**,** and **MBS430178** (MyBioSource) are mouse IgG monoclonal antibodies against the recombinant S1 of the MERS-CoV spike protein. The immunogen was DNA vaccine expressing recombinant S1 spike protein of the human betacoronavirus 2c EMC/2012 (aa 18-725, GenBank accession # AFS88936).
5. **MERS-S1-015** (eEnzyme) is a rabbit polyclonal antibody against the full length recombinant S1 spike protein of MERS-CoV. The immunogen was the aa 1-725 of GenBank accession # AFS88936.
6. **CABT-B1954** (Creative Diagnostics) is a rabbit IgG polyclonal antibody against MERS-CoV spike protein. The immunogen was a synthetic peptide corresponding to the N-terminus of the S1 subunit of MERS-CoV spike glycoprotein.
7. **CABT-B1954** (Creative Diagnostics) is a rabbit IgG polyclonal antibody against the MERS-CoV spike protein. The immunogen was a recombinant spike protein aa 1-725 of the MERS-CoV.

***In vitro* detection of purified MERS-CoV spike proteins with rabbit polyclonal antibodies**

We tested the three different rabbit polyclonal antibodies for their ability to bind to the three different MERS-CoV spike proteins (see Table 3) *in vitro*. The results show that all three polyclonal antibodies (pAb 1, 2, 3) could bind the spike protein. Further, in all three cases pAb 3 appeared to bind more strongly, as reflected by the strongest fluorescence signal that resulted in assays with pAb 3 (Figure 27). Bovine serum albumin (BSA) was included as negative control, which showed little to no RFU.

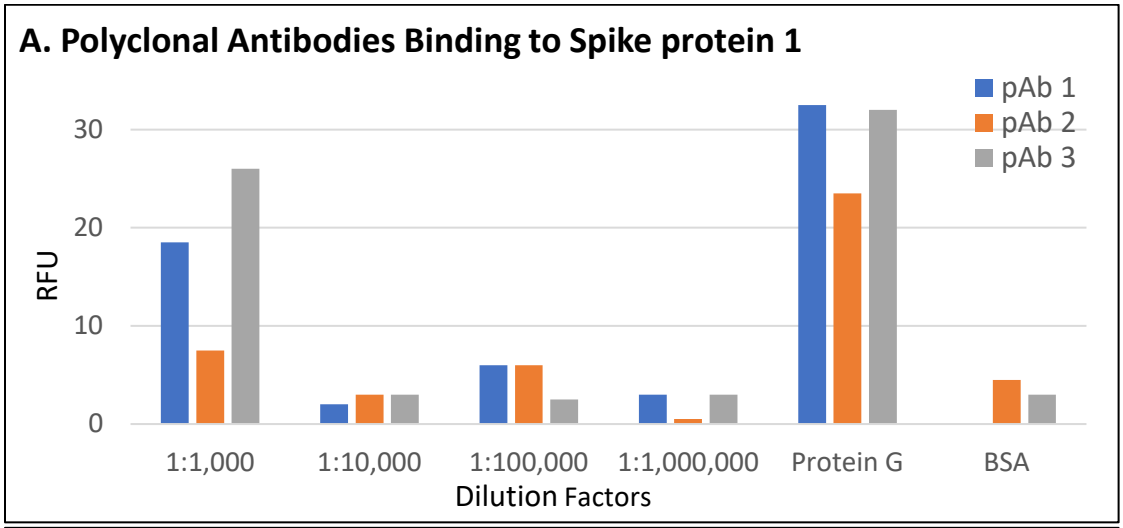


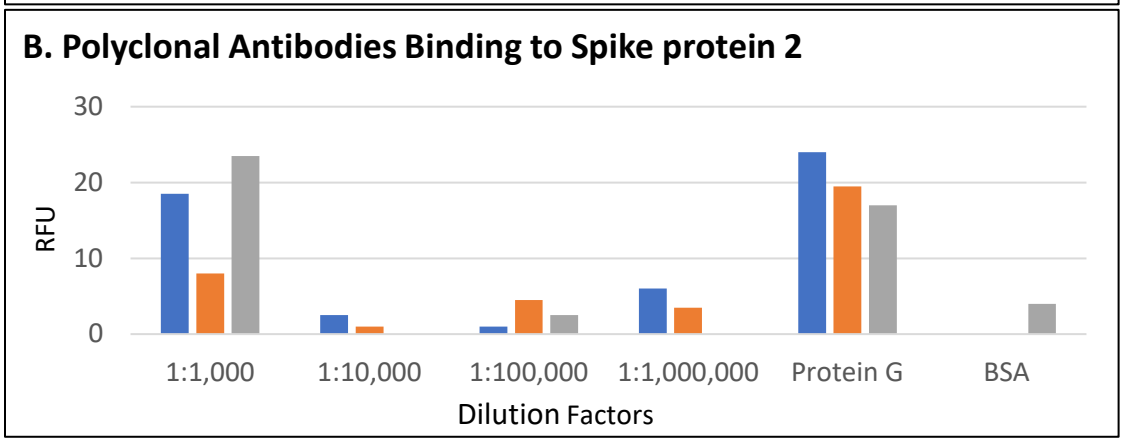

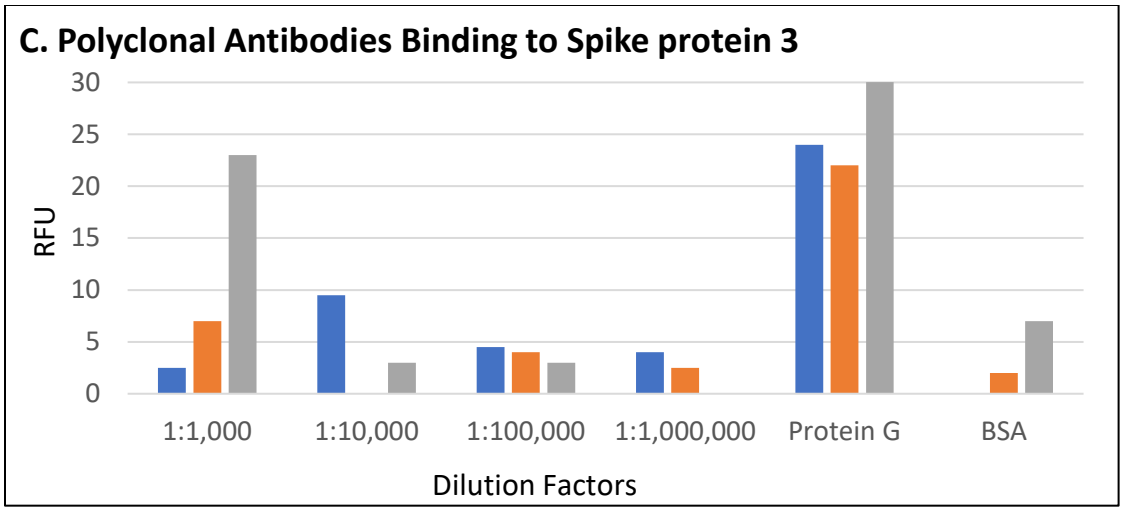


**Figures 27. Analysis of three different rabbit polyclonal antibodies (pAb1, -2, -3) against three different MERS-CoV spike proteins (see Table 3)**. **A,** spike protein 1. **B,** spike protein 2. **C,** spike protein 3. Black ELISA plates were separately coated with each spike protein at 2 µg/mL in carbonate-bicarbonate buffer. The plates were washed to remove free, residual spike proteins, the rabbit polyclonal antibodies were added, washed, and then incubated with Alexa Fluor® 647 conjugated goat anti-rabbit IgG. The plates were washed again to remove unbound secondary antibodies, followed by fluorescence reading with BioTek Synergy H1 plate reader. The excitation wavelength was set at 638 nm, emission wavelength at 668 nm, and gain at 100.

***In vitro* detection of purified MERS-CoV spike proteins with mouse monoclonal antibodies**

We also evaluated three different monoclonal antibodies for detection of the three MERS-CoV spike proteins described in Table 3. To do that, the plates were separately coated with each of the three spike proteins, and the three monoclonal antibodies were then evaluated for binding to the immobilized spike proteins. We found that all three mAbs, like the three pAbs (Figure 27), could bind the spike proteins (Figure 28). The results further show that overall mAb 1 bound the spike proteins more strongly than mAb 2 or 3, except at 1:500 dilution, in which case mAb 2 bound more strongly (Figure 28). Protein G was included as positive control for the assay, and BSA as a negative control.

We further evaluated mAb 1 and mAb 2 for detection of spike protein 1, except that in these assays we coated the plates with the mAbs and used spike protein 1 for binding to the immobilized mAbs. In these assays, mAb 1 consistently generated stronger fluorescence signals in the spike protein 1 concentration range of 12.5 to 400 ng/mL, suggesting mAb 1 interaction with spike protein 1 is stronger than with mAb 2 (Figure 29). We therefore decided to use mAb 1 for the remainder of the study.

Generally, in our assays, spike protein 1 interactions with both the pAbs and mAbs elicited stronger fluorescence signals, and for that reason we decided to use this spike protein for the remainder of the work.

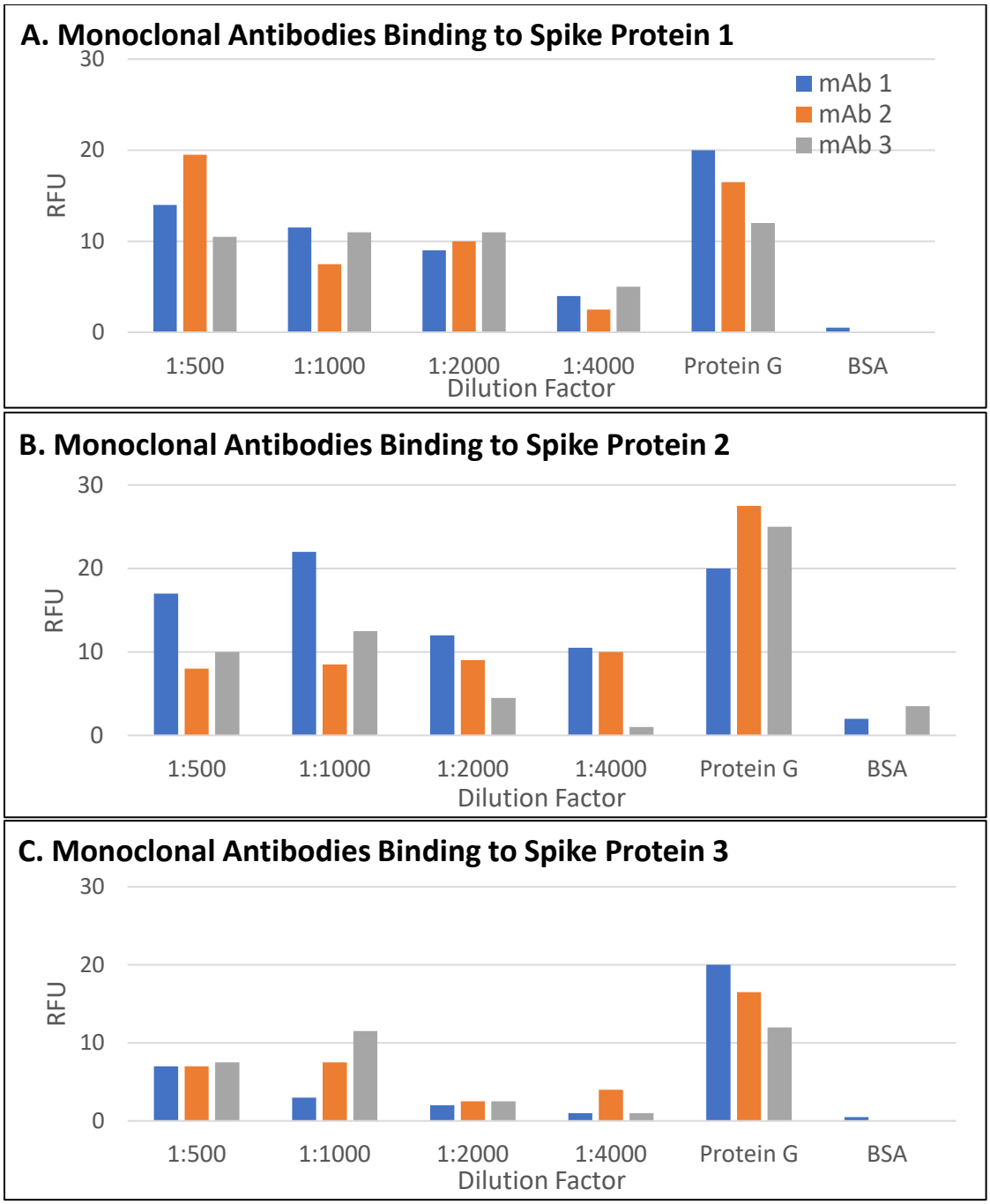


**Figures 28. Analysis of the three mouse monoclonal antibodies (mAb1, -2, -3) against three different MERS-CoV spike proteins (see Table 3). A**, spike protein 1**. B**, spike protein 2**. C**, spike protein 3. Black ELISA plates were separately coated with each spike protein at 2 µg/mL in carbonate-bicarbonate buffer. The plates were washed to remove free, residual spike proteins, the mouse monoclonal antibodies were added, washed, and then incubated with Alexa Fluor® 647 conjugated goat anti-mouse IgG. The plates were washed again to remove unbound secondary antibodies, followed by fluorescence reading with BioTek Synergy H1 plate reader. The excitation wavelength was set at 638 nm, emission wavelength at 668 nm, and gain at 100.

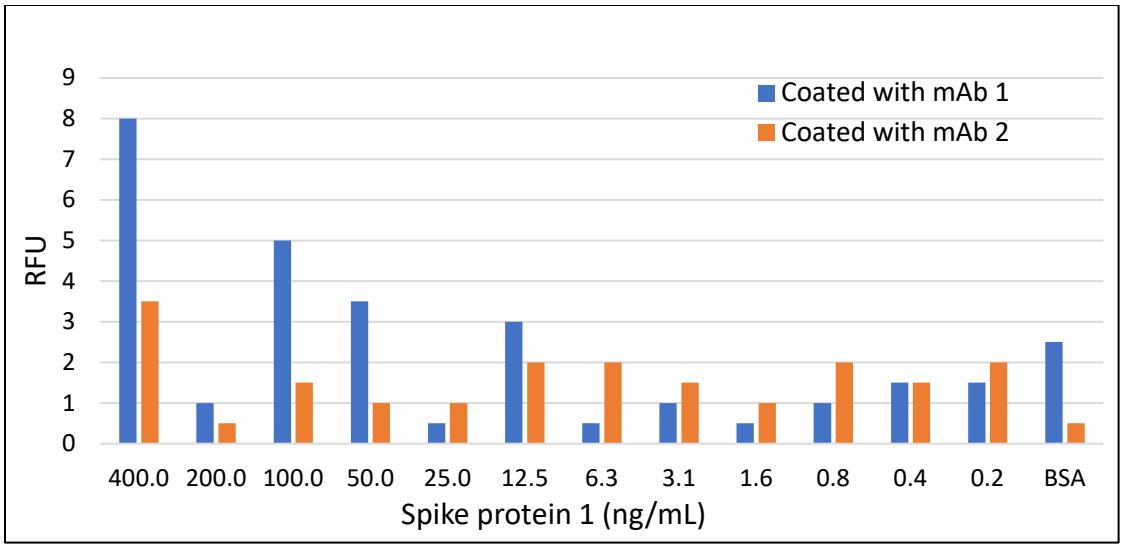


**Figure 29. FLISA analysis of the binding of mAb 1 vs. mAb 2 to spike protein 1**. Black ELISA plates were coated with mAb 1 or mAb 2 at 2 µg/mL in carbonate-bicarbonate buffer. The plates were washed to remove free, residual antibodies. Spike protein 1 was added at different concentrations, incubated, and washed while the pAb 3 was added, washed, and then incubated with Alexa Fluor® 647 conjugated goat anti-rabbit IgG. The plates were washed again µµto remove unbound secondary antibodies, followed by fluorescence reading with BioTek Synergy H1 plate reader. The excitation wavelength was set at 638 nm, emission wavelength at 668 nm, and gain at 100. BSA was included as negative control.

**Optimization of the FLISA**

We tested different experimental conditions to optimize the FLISA. The aim was to improve the fluorescence detection limit of the spike protein while maintaining the low background signal. First, we tested different concentrations of the coating mAb to see if a higher concentration of the mAb would lead to more binding of MERS-CoV spike protein. We tested mAb concentrations from 2 to 8 µg/mL. BSA (2 µg/mL) was included as a negative control. The assay revealed 2 to 4 µg/mL of the mAb to be sufficient (Figure 30).

Next, we tested two different buffers, phosphate buffered saline (PBS, pH 7.2) and carbonate-bicarbonate buffer. The results did not appear to suggest one or the other buffer to be better in these assays (Figure 30). We decided to use PBS as the coating buffer for the rest of the experiment.

Last, we set the BioTek Synergy H1 spectrophotometer at different gain values – 100, 125, 140, and 150 – to see which setting afforded the strongest fluorescence readings. The excitation and emission wavelengths were kept constant at 638 nm and 668 nm, respectively. We did not test gain value above 150 as that was not recommended by the manufacturer. The results show that the gain value of 150 produced more than 15-fold higher RFU than gain value of 100 (Figure 30).

Furthermore, there was no appreciable increase in background noise fluorescence readings from samples with BSA with gain setting at 150 (Figure 30).

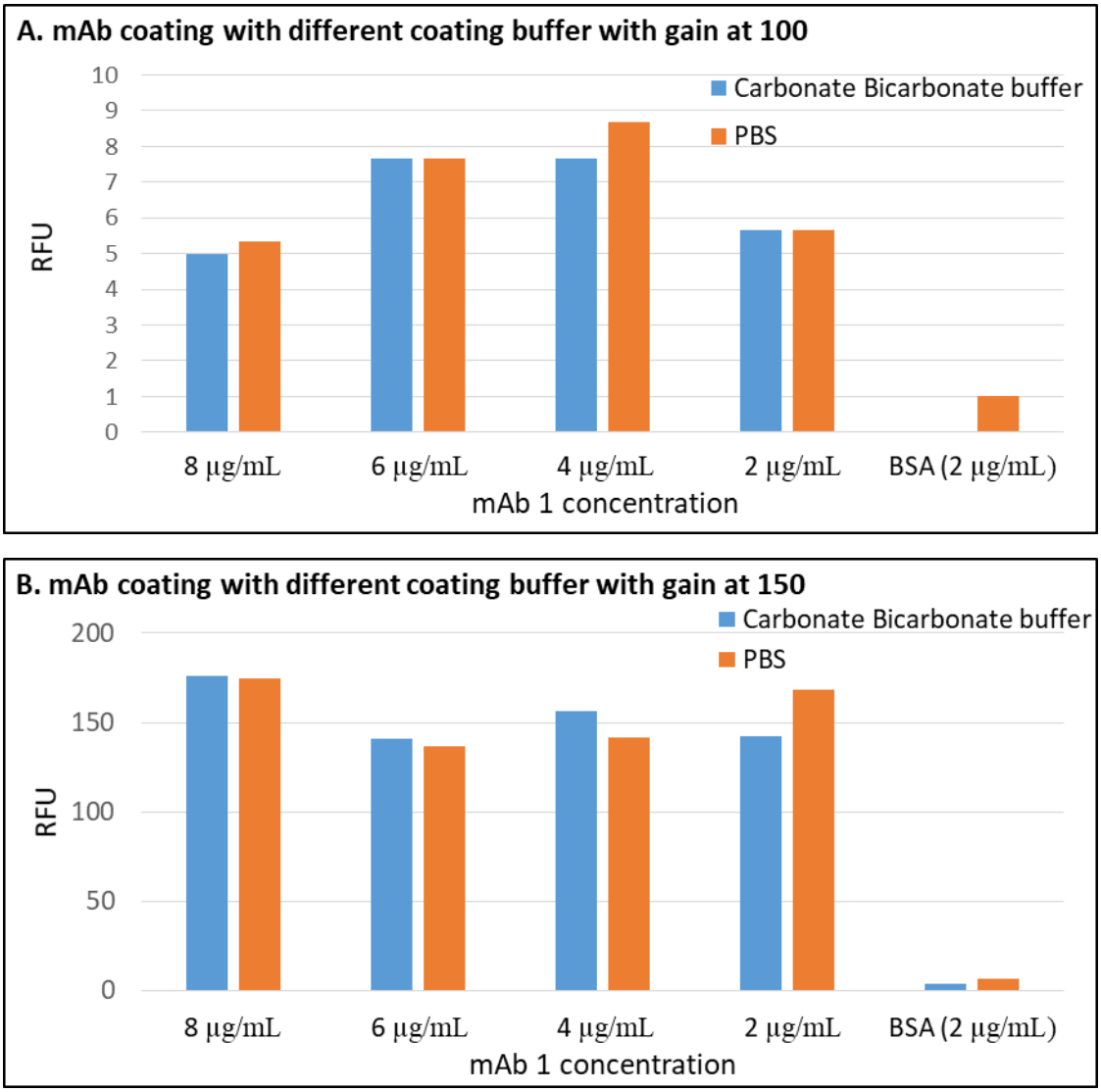


**Figure 30. Analysis of different FLISA conditions for the detection of MERS-CoV spike protein.** **A.** Reading with gain 100**. B.** Reading with gain 150**.** Plate was coated at different concentrations of mAb in PBS or carbonate-bicarbonate buffer. Procedure was as described in Figure 27. Fluorescence reading was done with BioTek Synergy H1 reader at excitation wavelength of 638 nm, emission wavelength of 668, and gain of 100, 125, 140 and 150. Data for gain at 125 and at 140 were not shown.

**Testing reagents after FLISA optimization**

After optimizing the assay conditions, we repeated the screening assay to ensure that the reagents performed as expected under the optimal conditions, listed below:

- Using 2 µg/mL of protein for coating plates
- Using PBS as the buffer
- Excitation and emission wavelength settings at 638 nm and 668 nm, respectively, for fluorescence readings of Alexa Fluor® 647 conjugated antibodies
- BioTek Synergy H1 gain setting at 150

FLISA performed under these conditions showed that all three monoclonal antibodies detected spike protein 1, but that mAb 1 and mAb 2 gave stronger signals than mAb 3 (Figure 31). In a similar assay that employed the three pAbs to detect spike protein 1, we found that pAb3 gave stronger signals, although pAb1 and pAb2 also generated sufficient signals (Figure 32).

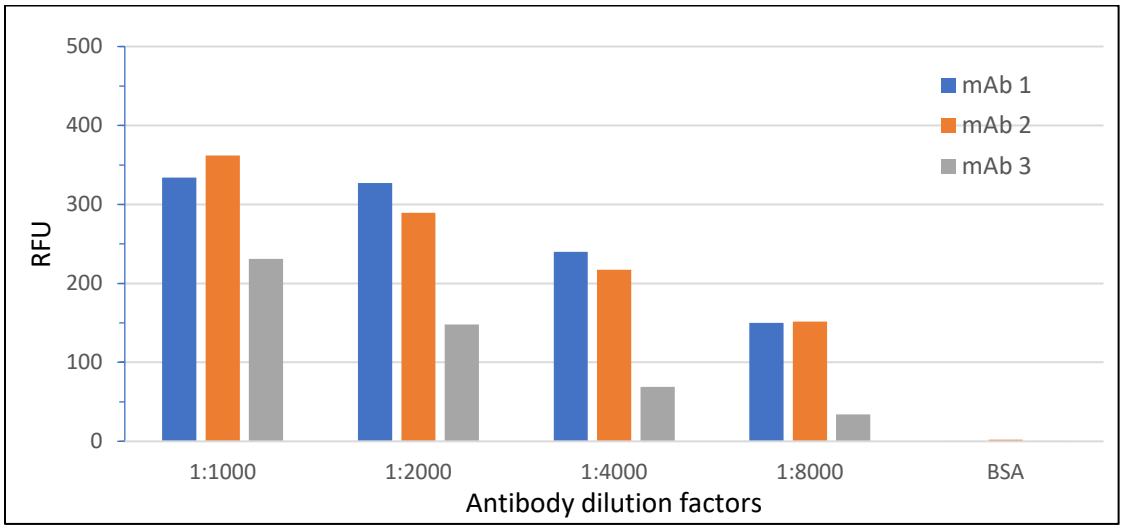


**Figure 31. Analysis of the three monoclonal antibodies against the MERS-CoV spike protein 1 under optimal assay conditions.** Black ELISA plate was coated with spike protein 1 at 2 µg/mL in PBS. The plate was washed to remove free, residual spike proteins, the rabbit polyclonal antibodies were added, washed, and then incubated with Alexa Fluor® 647 conjugated goat anti-mouse IgG. The plate was washed again to remove unbound secondary antibodies, followed by fluorescence reading with BioTek Synergy H1 plate reader. The excitation wavelength was set at 638 nm, emission wavelength at 668 nm, and gain at 150.

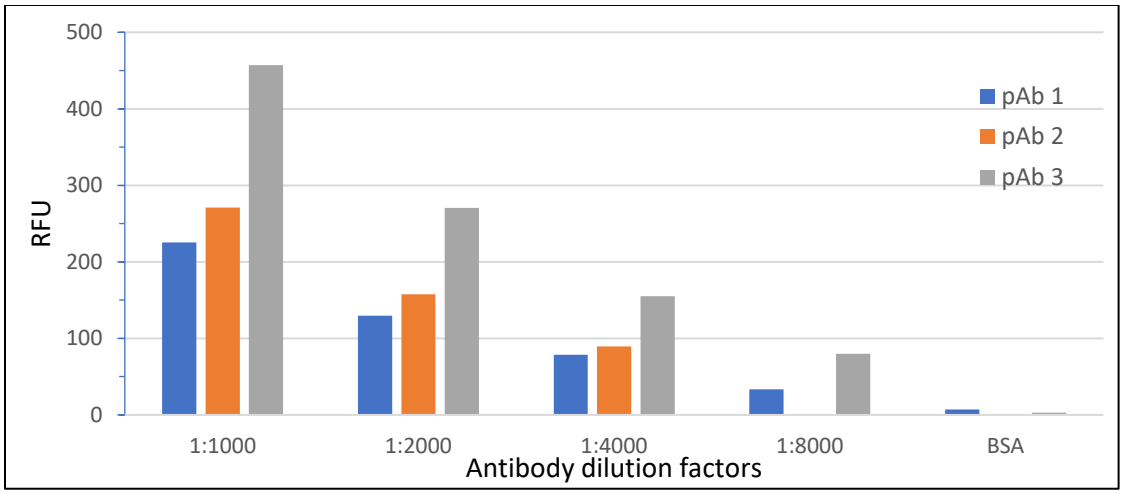


**Figure 32. Analysis of the three polyclonal antibodies against the MERS-CoV spike protein 1 with new assay conditions.** Black ELISA plate was coated with spike protein 1 at 2 µg/mL in PBS. The plate was washed to remove free, residual spike proteins, the rabbit polyclonal antibodies were added, washed, and then incubated with Alexa Fluor® 647 conjugated goat anti-rabbit IgG. The plates were washed again to remove unbound secondary antibodies, followed by fluorescence reading with BioTek Synergy H1 plate reader. The excitation wavelength was set at 638 nm, emission wavelength at 668 nm, and gain at 150.

**FLISA limit of detection of MERS-CoV spike protein**

We tested the limit of detection of the FLISA at detecting MERS-CoV spike protein with the BioTek Synergy H1 reader. The results show that the assay can reliably detect 25 ng/mL of MERS-CoV spike protein (Figure 33). We considered detection readings reliable if they were at least about 2-fold greater than the background or negative control readings (BSA, no spike protein).

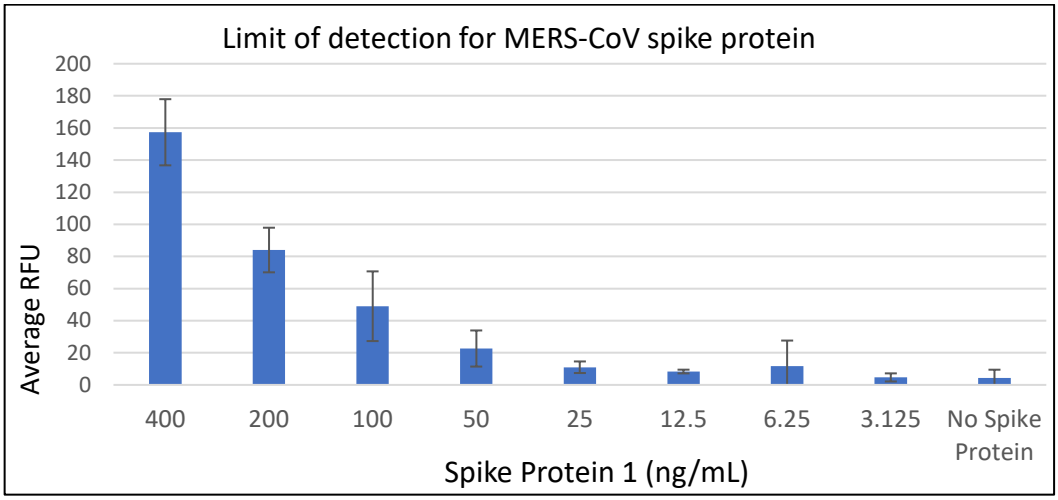

**Figure 33. Limit of detection of MERS-CoV spike protein with the BioTek Synergy H1 reader.** The RLU were plotted as means, with standard deviations shown as error bars. The procedure was as described in Figure 29 with the gain setting at 150.

## Testing of the fluorescence detection capability of the goggle prototype

### Big vs. small lens

The goggle prototype came with two different lens sizes, 21 mm, and 8 mm. We tested the two lenses to see which performed better at detecting fluorescence signal by measuring the fluorescence signal of the Alexa Fluor® 647 goat anti-rabbit IgG at various concentrations. The data show that the 21-mm lens proved more sensitive at detecting the fluorescence signal than the 8-mm lens. The background fluorescence levels for the two lenses were about the same (Figures 34 and 35).

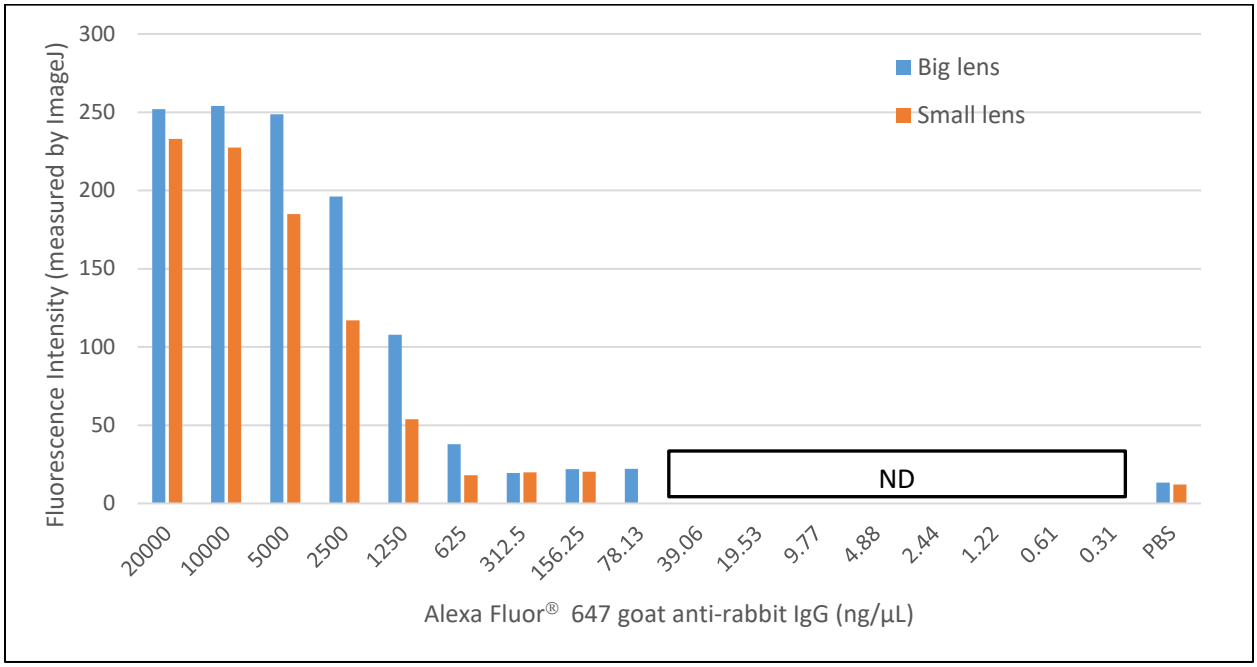


**Figure 34. Fluorescence detection capability of the goggle with big vs. small lens (21 mm vs. 8 mm)**. Alexa Fluor® 647 goat anti-rabbit IgG was prepared in PBS at various concentration in a black 96-well ELISA plate. The handheld light source with the highest illumination setting was used as the excitation light source. The goggle was mounted approximately 12 inches directly above the plate. The goggle prototype was set to capture images at 15 frames per second (fps). The fluorescence intensity of each sample was measured by ImageJ from the captured images. ND - No measurement was made from the captured images with ImageJ.

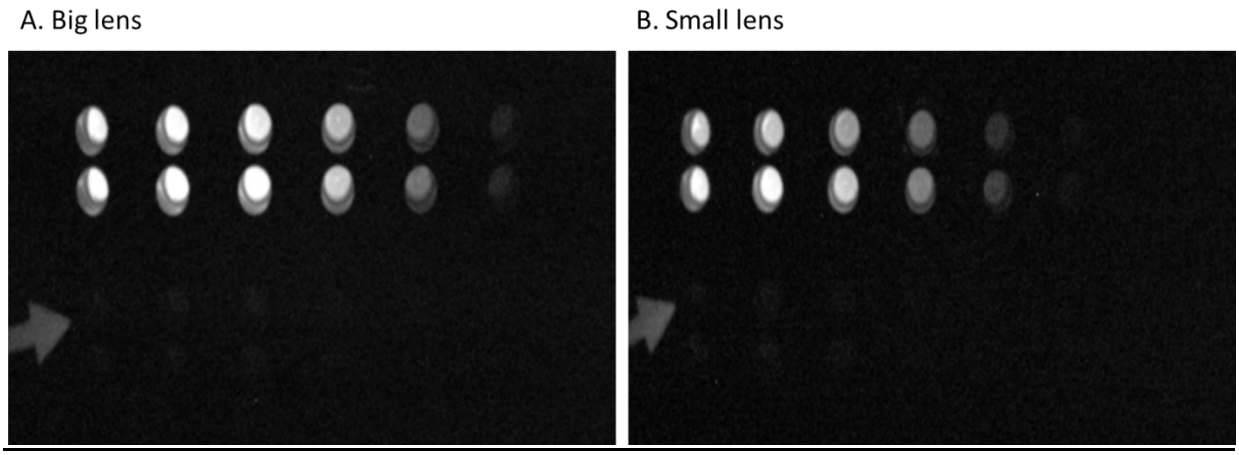


**Figure 35. Fluorescence images captured with the goggle prototype equipped with big lens (A) and small lens (B).** The handheld light source with the highest illumination setting was used for the excitation. The goggle prototype was mounted approximately 12 inches directly above the samples. Images were captured at 15 fps.

**Fluorescence sensitivity of the goggle prototype with different fps setting**

The goggle prototype is capable of capturing fluorescence images at variable fps. Greater numbers of fps translate to longer exposure time. This, in turn, should result in higher fluorescence sensitivity. We tested the goggle prototype with 5, 10, or 15 fps. The data indicated that capturing images at 5 fps offered the most fluorescence sensitivity (Figure 36). The fluorescence detection limit was about 2-fold greater when comparing the 5 fps to 10 fps or 15 fps setting. Fluorescence signal appeared to be saturated at the 5000 ng/mL.

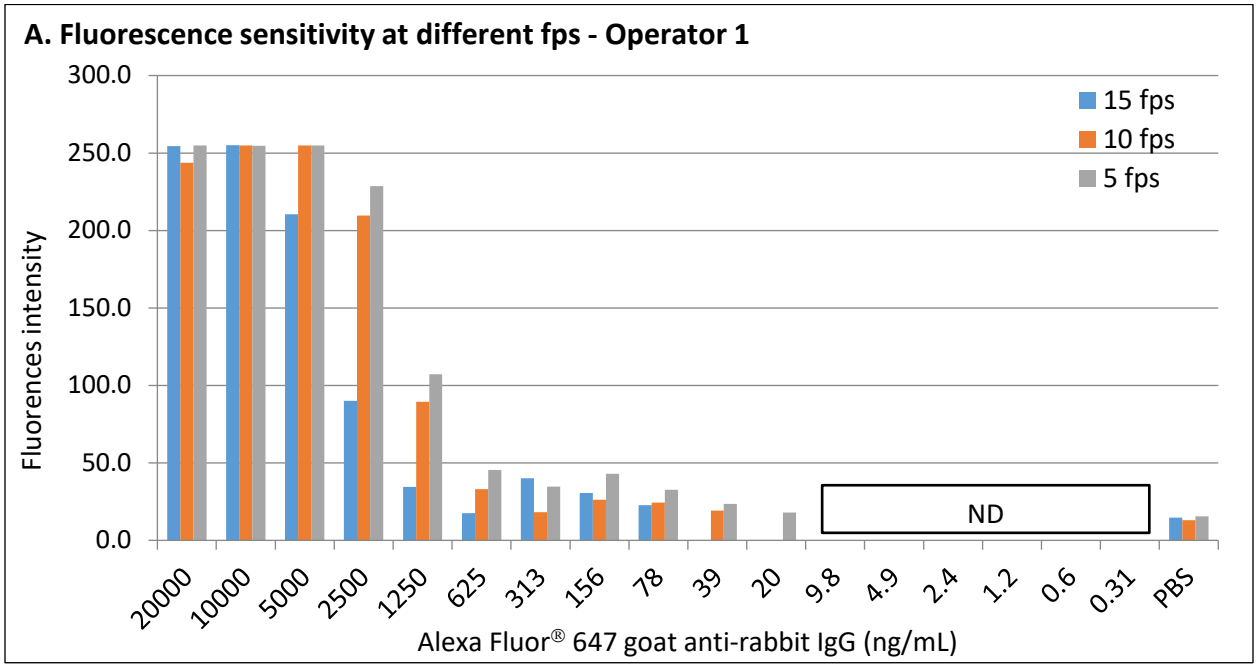

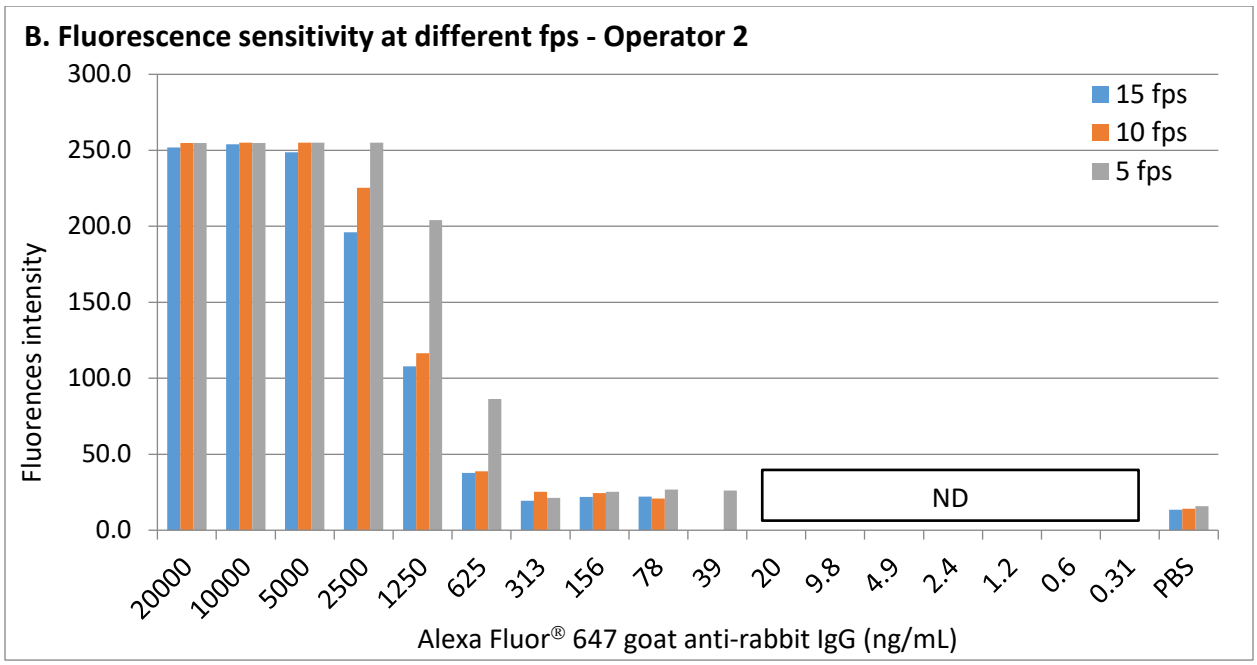


**Figure 36: Fluorescence detection capability of the goggle prototype at different fps settings for operator 1 (A) and operator 2 (B).** All images were captured with the big lens. Experimental procedure was as described in Figure 34. ND, no measurement was made from the captured images with ImageJ.

**<u>Fluorescence sensitivity of the goggle prototype vs BioTek Synergy H1 reader</u>**

For the fluorescence sensitivity comparison between the goggle prototype and the BioTek Synergy H1 reader, we prepared 2-fold serial dilutions of the Alexa Fluor® 647 IgG in a 96-well black plate. The concentration ranged from 0.31 to 20,000 ng/mL. The results show that the fluorescence detection limit of the BioTek Synergy H1 reader was 20 ng/mL and 4.9 ng/mL of the Alexa Fluor® 647 IgG for operator 1 and 2, respectively (Figure 37A). The fluorescence detection limit of the goggle prototype was 625 ng/mL and 78 ng/mL for operator 1 and 2, respectively (Figure 37B). As in other assays described above, we considered fluorescence signals reliable if they were at least about twice as high as the background level. The data show that the BioTek Synergy H1 reader is at least 15-folds more sensitive than the goggle prototype at detecting fluorescence signal.

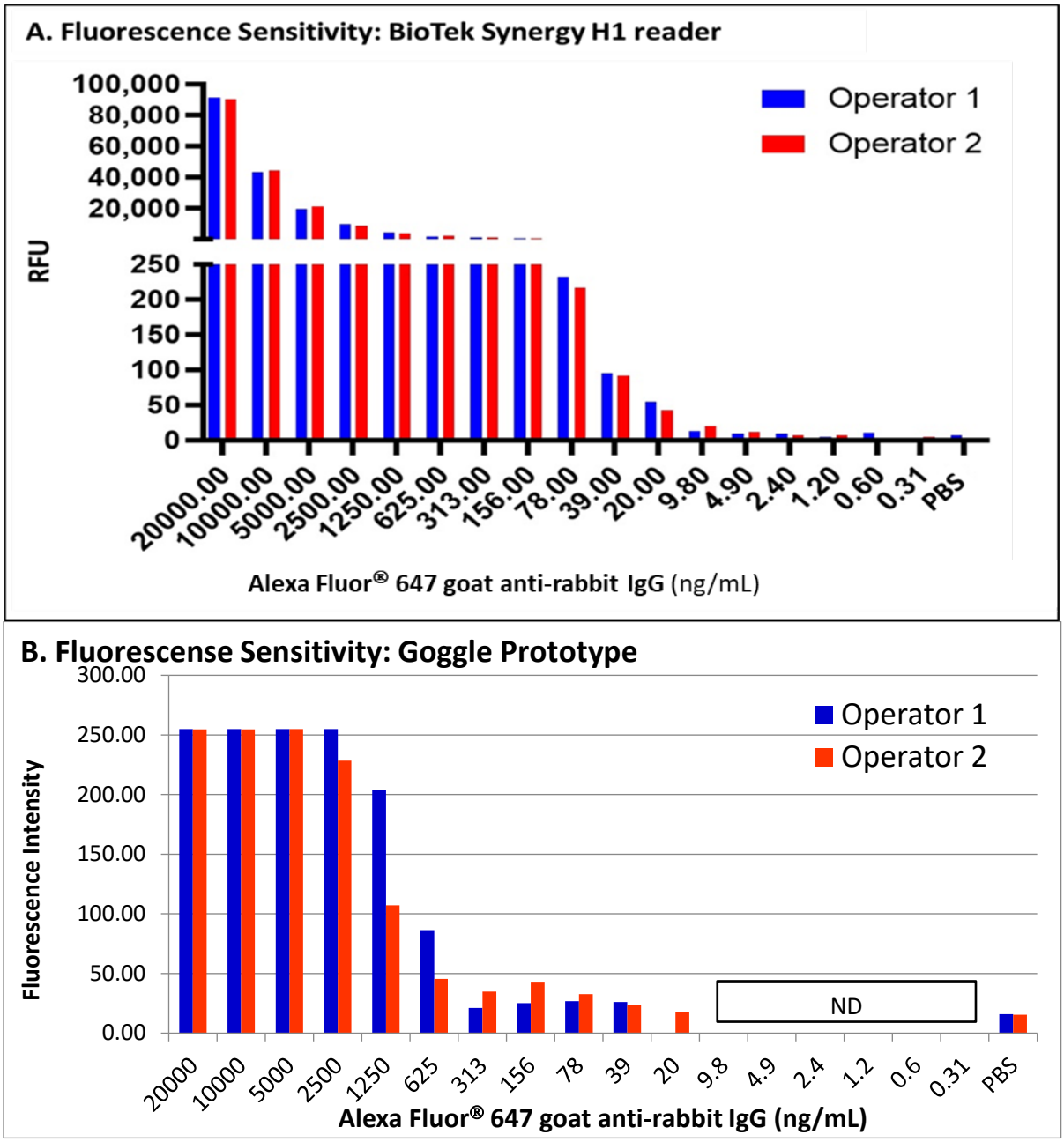


**Figures 37. Fluorescence sensitivity of the BioTek Synergy reader (A) vs the goggle prototype.** Alexa Fluor® 647 goat anti-rabbit IgG was diluted with PBS in black ELISA plate. The experiments were independently performed by 2 operators. **A:** The BioTek Synergy H1 reader measured fluorescence intensity as RFU. **B:** Fluorescence intensity was measured by ImageJ from images captured by the goggle prototype. The handheld light source with the highest illumination setting was used for the fluorescence excitation. The goggle was mounted at approximately 12 inches directly above the plate. Images were captured at 5 fps with big lens. PBS was included for the background fluorescence level. ND, no measurement was made from the captured images with ImageJ.

We also qualitatively analyzed the captured images (Figure 38). With unaided eyes we recorded a "+" for samples that we could distinguish from the background noise (brighter than the background) or "-" for samples that we could not distinguish from the background noise (Table 4). Based on this analysis, the fluorescence detection limit of the goggle prototype was 39 ng/mL of the Alexa Fluor® 647 IgG. This indicated that the BioTek Synergy H1 reader is >2-folds more sensitive than the goggle prototype at detecting fluorescence signal.

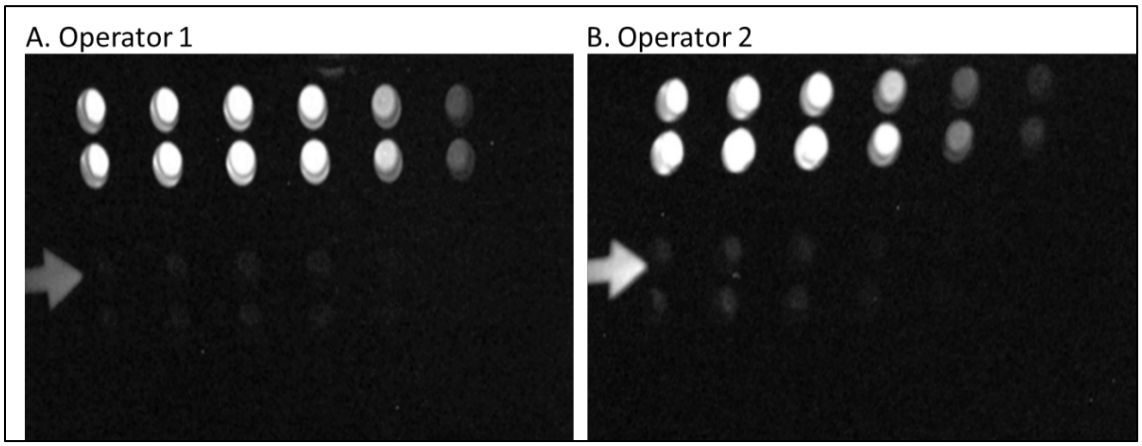


**Figure 38**. **Fluorescence images captured by the goggle prototype.** Handheld light source with the highest illumination setting was used for the fluorescence excitation. Images were captured at 5 fps using the goggle prototype equipped with big lens. The goggle prototype was mounted approximately 12 inches directly above the samples.

**Table 4. Qualitative assessment of the captured fluorescence images as shown in Figure 38.**

| Antibody Conc. (ng/mL) | 20000 | 10000 | 5000 | 2500 | 1250 | 625 | 313 | 156 | 78 | 39 | 20 | 9.8 | 4.9 | 2.4 | 1.2 | 0.6 | 0.3 | PBS |
|---|---|---|---|---|---|---|---|---|---|---|---|---|---|---|---|---|---|---|
| Operator 1 | + | + | + | + | + | + | + | + | + | + | - | - | - | - | - | - | - | - |
| Operator 2 | + | + | + | + | + | + | + | + | + | + | - | - | - | - | - | - | - | - |

**Notes:** A "+" indicated that difference in fluorescence brightness level between the sample and the background can be distinguished by unaided eyes. A "-" indicated that there was no differences.

**<u>The goggle prototype and the MERS-CoV spike protein detection</u>**

We ran FLISA for the detection of purified MERS-CoV spike protein as described in the material and method section. The plates were read by both the BioTek Synergy H1 reader and the goggle prototype. The Synergy H1 Hybrid reader was able to detect the fluorescence signal at 3.13 ng/mL and 12.5 ng/mL of the of the MERS-CoV spike protein for operator 1 and 2, respectively (Figure 39A). The goggle prototype, however, was not able to detect a positive fluorescence signal from any of the MERS-CoV spike protein concentrations (Figure 39B). Note that we defined a positive fluorescence signal as having a reading of at least 2 times that of the background fluorescence signal. However, the goggle prototype was able to detect weak

fluorescence signal (Figure 39C). With unaided eyes, we could distinguish samples that contained spike protein from the samples that did not contain any spike protein or the background noises.

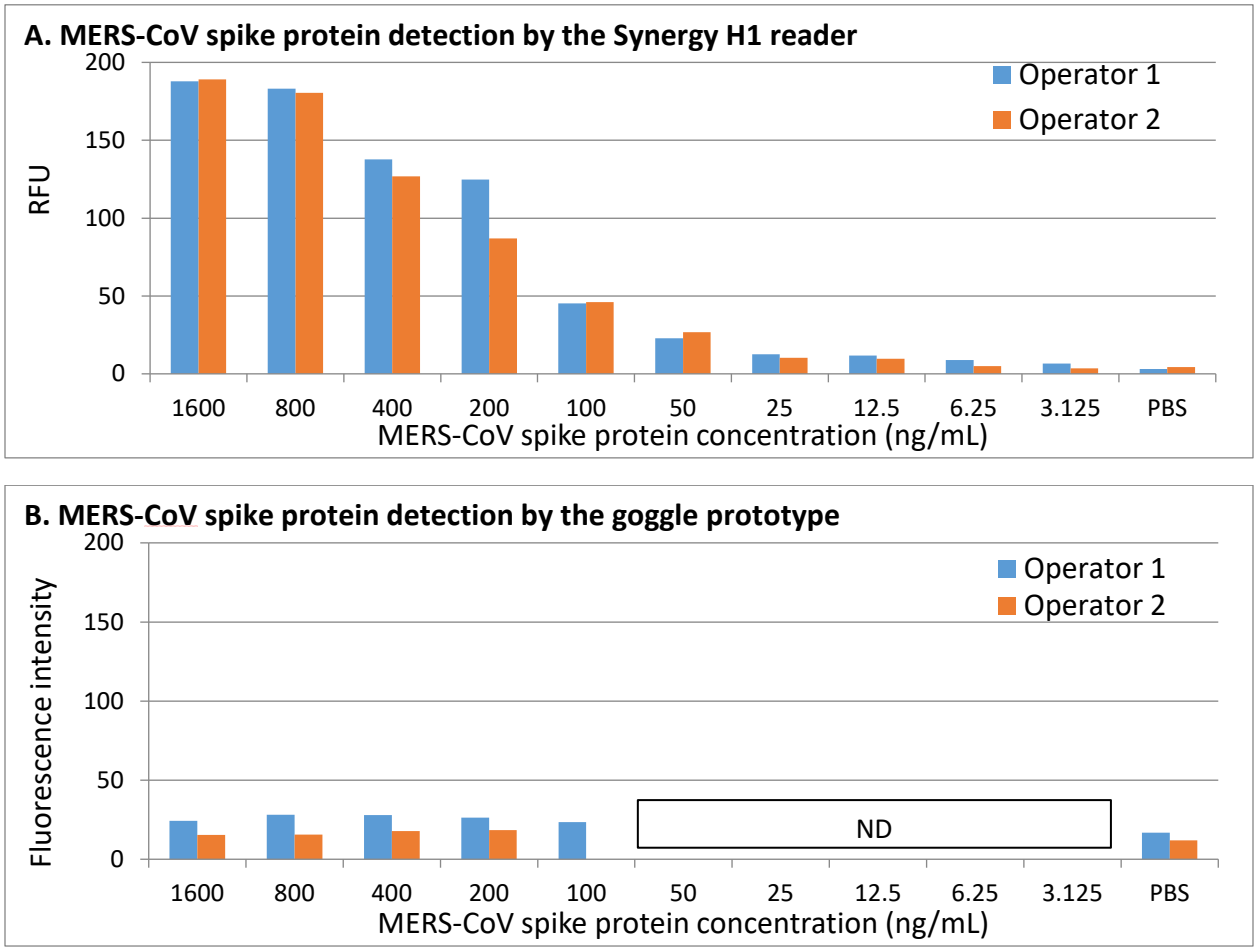


**C. Captured goggle prototype image**

**Figure 39. The goggle prototype vs the plate reader at detecting MERS-CoV spike protein.** The FLISA was performed as described in the material and method section. The assays were

performed independently by 2 different operators. **A,** Data was obtained from the Synergy H1 reader with excitation at 638, emission at 668, and gain at 150. **B,** Data obtained from ImageJ by measuring the brightness from the images captured by the goggle prototype. **C,** Fluorescence image that was captured by the goggle prototype. Handheld light source with the highest illumination setting was used for the fluorescence excitation. The image was captured at 5 fps with the goggle prototype equipped with the big lens. The goggle was mounted approximately 12 inches directly above the samples. ND, no measurement was made from the captured images with ImageJ

**Raman spectroscopy capability of the goggle prototype**

We were not able to assess the Raman spectroscopy capability of the goggle prototype because the capability was not ready for testing when CAMD received the goggle prototype.

## Change of Institution of University of Akron Team

Dr. Yang Liu and his research assistants (Maziyar Askari & Tri Quang) moved to the University of Iowa starting January 2019. Dr. Liu has been promoted to associate professor in Electrical and Computer Engineering at the University of Iowa; Maziyar Askari & Tri Quang have been accepted into the PhD program in Electrical and Computer Engineering at the University of Iowa. The change of institution concluded the project 6 months prior to the project deadline and saved $176,071 cost from the original budget. The remaining unused portion of budget was returned to AFRL.

## Technology readiness level (TRL) Assessment

In addition, Dr. James Rader from BlueRidge Federal Consulting has conducted the TRL assessment on behalf of AFMSA/SG5. The goggle is assessed to be an achieved TRL3 and an emergent TRL 4. The report was submitted to Mr. McCarty and Mr. Walter at AFMSA.

# TRA Summary: Goggles in a Clinical Setting

**About this technology:** Current techniques for identifying pathogens involve sample preparation prior to inserting the sample into a PCR or similar device to confirm the existence of the pathogen in the sample. By eliminating sample preparation, the identification process can be much quicker. If the sample can be tagged with a fluorescent marker, goggles (which are tuned to the wavelength of the marker) can make detection very quick. Once the presence of the pathogen is confirmed, treatment can begin immediately and measures can be taken to prevent its spread. Goggles that are under development by the University of Akron are being tested to perform this task. The goggles detect the fluorescence emitted by the marker and make it visible to the person wearing the goggles.

**Actions required to Mature Technology:**

- Establish customer requirements with thresholds & objectives
- Complete prototype and bring to scale
- Start interaction with FDA (Can Novadaq device be considered predicate device to streamline FDA process?)
- Conduct preliminary testing & evaluation
- Develop Risk Management Index
- Establish quality & reliability baseline

**AFMS R&D Action Items:**

- ❑ *Assist 59 MDW with customer ID and requirements development*
- ❑ *Provide FDA review and guidance*
- ❑ *Plan/Program for FY19-20*
- ❑ *Develop long range acquisition strategy (how many, who, how)*
- ❑ *Alert and resource MILTECH for potential FY20 support of manufacturing planning & optimization to start-up company*

| Eval Date | Achieved TRL | Emergent TRL(s) |
|---|---|---|
| Sep-2017 | 3 | 4 |

**R&D Context:** Initial work on the Goggle platform began in 2012 but the application was to assist in surgery. The application for pathogen detection began in September 2016. The surgical platform currently has three IRB approved trials on-going at the Cleveland Clinic. The pathogen prototype will be delivered to 59 MDW early in 2018 for testing. It is anticipated that an additional two years are required to deliver an approved clinical version of the Goggle. The University of Akron will license the technology to a start-up company to complete development (with 59 MDW DT&E support), FDA approval and manufacturing.
**Associated Vendor(s):** University of Akron - http://www.uakron.edu
**AF R&D Lead Org:** 59 MDW (Mr. Manny Caballero)
**Researcher(s):** Dr. Yang Liu, University of Akron
**Champion(s):** 59 MDW
**Customers:** None engaged at this time —ACC, AFSOC, Military Treatment Facilities are potential customers
**Tech Push/Pull:** Push
**Requirement:** 2015 ICL #15 "Rapid Tests for Specific Disease Outbreak/Surveillance"; this could contribute to that capability
**AFMS Funds Required:** Current funds ($525K) deliver prototype to 59 MDW for testing. To achieve TRL 9 (including FDA approvals if/as req) BlueRidge ROM estimate is $1.5M needed through FY20 (assuming minimal FDA compliance work required if Novadaq is indeed predicate)
**Acquisition Support Required:** Possible (depends on customer need)
**Portfolio Mgr Support Required:** Plan for continued funding
**Manufacturing Support Required**: Yes – consulting support to company
**ORTA Support Required:** No
**T&E Support Required:** Possible support for OT&E
**FDA Support Required:** Possible (depending on use cases)
**Other Notes:**

*Breaking Barriers … Since 1947*

2

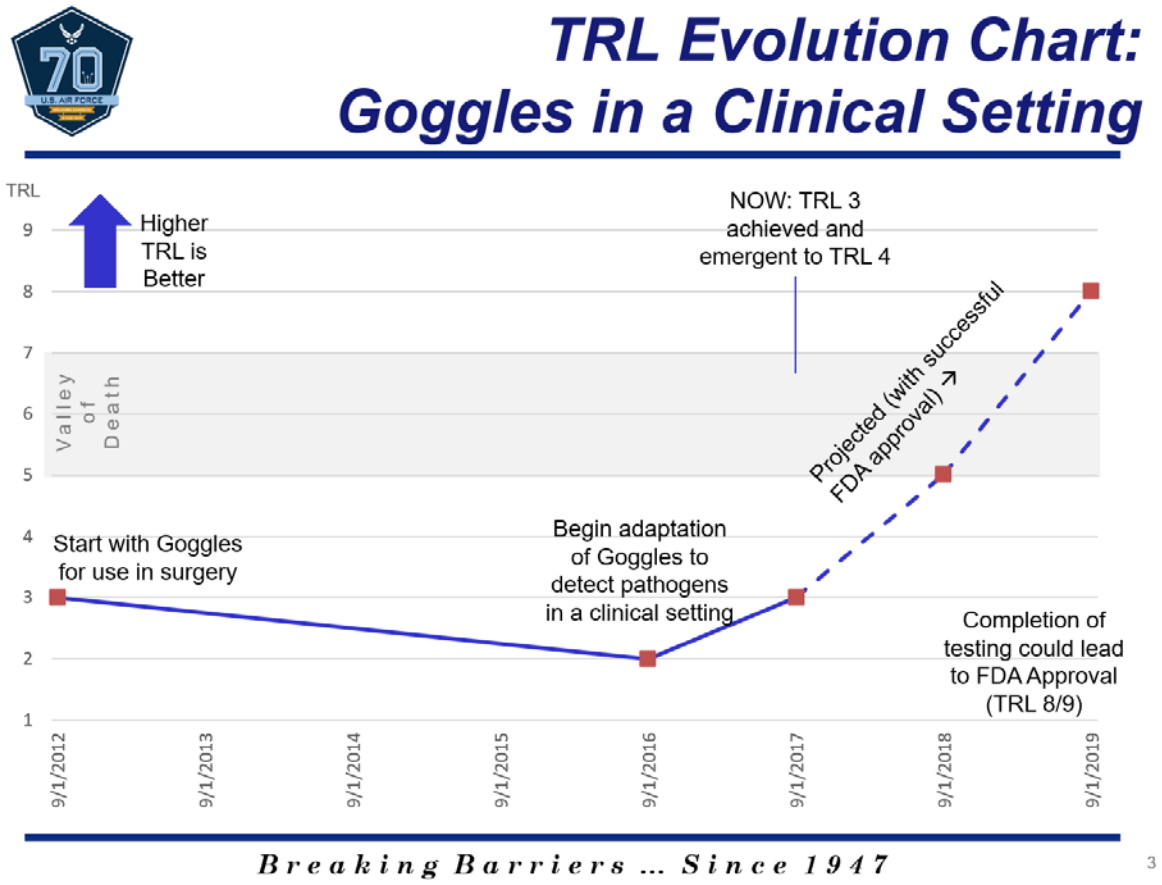


**Figure 40.** TRL assessment performed by Dr. Rader at BlueRidge Federal Consulting.

**SUMMARY**

1. The overall goal of this project was to develop, test, and evaluate a novel platform technology capable of sensitive, real-time detection of MERS-CoV. For this project only *in vitro* assays with purified MERS-CoV spike protein were performed.
2. The task objectives included: (a) Development of a prototype Multipurpose Imaging Goggle and fluorescence-based assay for detection of MERS-CoV and other viral or bacterial pathogens. (b) Conduct initial testing of the prototype Multipurpose Imaging Goggle and detection assay, optimize the prototype goggle and detection assay based on test results and user feedback, and develop a user-friendly software package. (c) Evaluate the Multipurpose Imaging Goggle as a platform technology for infectious disease threat identification and surveillance and determine the sensitivity and specificity of the viral or bacterial detection assay using the optimized Multipurpose Imaging Goggle.
3. The goggle device is at an achieved TRL3 and an emergent TRL 4, based on an independent assessment by BlueRidge Consultants that was conducted in September 2017.
4. Dr. Yang Liu and his team moved to the University of Iowa starting January 2019. The change of institution concluded the project 6 months prior to the project deadline and saved $176,071 cost from the original budget.
5. Imaging, illumination, display, analysis, and control modules have been developed for the the pathogen screening goggle prototype.
6. Individual modules have been integrated to produce a prototype goggle. The prototype has been characterized and optimized. A software package with graphic user interface was also developed.
7. SmartGoggle software was not fully developed for quantitative or qualitative analysis of data, due to change of institution.
8. Goggle prototype had too many wires and too bulky for any field applications. Computer was a desktop with monitor connected to goggle prototype which initially had a mounted light source with a tripod. This was later reduced to a hand-held light device.
9. Goggle prototype offers high fluorescence imaging resolution (0.01 mm resolution), a high dynamic range, and detects fluorescence down to 0.5 nM concentration in microtubes.
10. Goggle prototype was able to detect fluorescence signal in microtubes well but suffered when capturing images in 96-well plate.
11. Using FLISA for detect purified MERS-CoV spike protein, the goggle prototype was not able to detect any positive samples. However, we were able to distinguish the samples containing the protein from the background.
12. The BioTek Synergy H1 Hybrid reader is laboratory equipment that allows us to benchmark the fluorescence detection capability of the goggle prototype. Our results showed that the goggle prototype was several times less sensitive in detecting fluorescence signal.

13. Both hardware and software modifications would need to be made to improve fluorescence sensitivity of the goggle prototype.
14. The Raman spectroscopy capability of the goggle prototype was not ready for testing when CAMD received the goggle prototype.
15. The project leads to multiple manuscripts. The knowledge generated from this project will be broadly disseminated to the DoD community.

**REFERENCES**


1. Darling RG *et al*. Threats in bioterrorism I: CDC category A agents. Emerg Med Clin N Am, 2002; 20, 273-309.
2. Liu Y. Multipurpose Imaging and Display System, 2014, PCT/US patent application: PCT/US2014/062454.
3. Liu Y. Imaging and Display System for Guiding Medical Interventions, 2014, PCT/US patent application: PCT/US2014/062468.
4. Abdel-Moneim A. Middle east respiratory syndrome coronavirus (MERS-CoV): evidence and speculations. Arch Virol, 2014; 159(7), 1575-1584.
5. https://www.cdc.gov/coronavirus/mers/about/symptoms.html
6. The Johns Hopkins Coronavirus Resource Center. Johns Hopkins University & Medicine. <https://coronavirus.jhu.edu/>
7. Mela CA, Patterson C, Thompson WK, Papay F and Liu Y. (2015) Stereoscopic Integrated Imaging Goggles for Multimodal Intraoperative Image Guidance, PLOS ONE, doi: 10.1371/journal.pone.0141956.